Numerical Analysis of Thermal Behavior and Fluid Flow in Geothermal Energy Piles

Willis Hope Thompson III

Thesis submitted to the faculty of the Virginia Polytechnic Institute and State University
in partial fulfillment of the requirements for the degree of

Master of Science
In
Mechanical Engineering

Srinath V. Ekkad, Chair
C. Guney Olgun
Michael Ellis
Joseph Wheeler

September 26, 2013
Blacksburg, VA

Keywords: Geothermal Energy Pile, Ground Source Heat Pumps

Numerical Analysis of Thermal Behavior and Fluid Flow in Geothermal Energy Piles

Willis Hope Thompson III

ABSTRACT

Geothermal heat exchangers are a growing energy technology that improve the energy efficiency of heating and cooling systems in buildings. Vertical borehole heat exchangers (BHE) coupled with ground source heat pumps have been widely developed and researched in the past century. The major disadvantage of BHEs is the initial capital cost required to drill the boreholes. Geothermal energy piles (GEP) were developed to help offset the high initial cost of these systems. A GEP combines ground source heat pump technology with deep earth structural foundations of buildings. GEPs are relatively new technology and robust standards and guidelines have not yet been developed for the design of these systems. The main operational difference between GEPs and conventional BHEs is the length and diameter of the below ground heat exchangers. The diameter of a GEP is much larger and the length is typically shorter than BHEs. Computational fluid dynamics (CFD) analysis is used in this study to investigate and better understand how structural piles perform as geothermal heat exchangers.

The CFD analysis is used to simulate an existing experimental energy pile test. The experimental test is modeled as built including fluid modeling to provide additional detail into the behavior of the circulation fluid within the pile. Two comparisons of large diameter GEPs are made using CFD analysis to gain knowledge of the effects of varying pile diameter and loop configuration. The thermal response test was successfully modeled using the CFD model. The CFD results closely match the results of the field test. The large diameter comparisons show that the performance of an energy pile will increase as

the diameter increases with a constant loop density. Multiple numbers of loops were tested in a constant diameter pile and the results show that with symmetrically placed loops the performance will increase with a greater number of loops in the pile.

ACKNOWLEDGMENTS

Along my journey through graduate school there have been many people who have helped me along the way to grow as a student, an engineer and a person. I would like to thank and acknowledge these people for their contributions to the completion of my graduate work. A sincere thank you to my graduate adviser Dr. Srinath Ekkad, he guided me through my master's program while offering encouragement and always challenged me to be better than I was before. In addition I would like to recognize the excellent help from Dr. Guney Olgun who always offered me advice and in depth discussion of ideas and concepts in the field of geothermal energy piles. Thank you to Professor Joe Wheeler who in the beginning of my graduate career enabled me to develop a plan of study that I was sincerely interested in and a special group of professors to work with along the way.

Thank you to Tolga Ozudogru whose research paralleled my own and helped me through my challenges and allowed me to better understand the underlying scientific principles. I would also like to thank all of the students in professor Ekkad's lab who were helpful in mastering the concepts of CFD and offered continuous support through graduate school.

A final sincere thank you to all of my friends and family for encouraging me and supporting my efforts. In particular my parents and my brother and sister who have always been there for me and who I could not have completed this program without.

TABLE OF CONTENTS

LIST OF FIGURES

LIST OF TABLES

LIST OF VARIABLES

A : Area

h : Integrating parameter

H : Pile Depth

k : Thermal Conductivity

Q : Rate of Heat Transfer

q : Heat Rate per Unit Length

R : Thermal Resistance

r : Radius

T : Temperature

t : Time

x : Distance

z : Coordinate in Depth

α : Thermal Diffusivity

γ : Euler's Constant = 0.5772…

Subscripts

f : fluid

p : pile

pw : pile wall

ACROYNMS

APGE Pile™	Auger Pressure Grouted Energy Piles
ASHRAE	American Society of Heating Refrigerating and Air Conditioning Engineers
BHE	Borehole Heat Exchanger
COP	Coefficient of Performance
FHWA	United States DOT Federal Highway Administration
GEP	Geothermal Energy Pile
GHSPA	Ground Source Heat Pump Agency
GSHP	Ground Source Heat Pump
GWT	Ground Water Table
HDPE	High Density Polyethylene
IEA	International Energy Agency
TC	Thermal Conductivity
TRT	Thermal Response Test

Chapter 1: Introduction

1.1 Background

The growing push for energy efficiency and sustainable energy systems has led to an increase in the use of ground source heat pumps (GSHPs) also referred to as ground coupled heat pumps. GSHPs are a sustainable alternative technology for the heating and cooling of buildings and homes in almost any climate [1]. A GSHP uses the thermal energy stored in the ground to transfer heat for heating or cooling purposes in buildings instead of conventional heat pumps, which use outdoor air. In North America and Europe GSHPs started being implemented in large numbers beginning in the 1970s and their use has been growing ever since [2]. Through the past decade the world has shown an annual increase of 16.6% in the installed capacity of these systems [3]. GSHPs can work effectively in most of the world's climates to provide space heating or cooling and domestic hot water [4]. The energy consumed by a GSHP can typically deliver three to four times as much thermal energy as electrical energy consumed to operate the pumps and compressor [4]. In addition to being efficient, GSHPs have very low maintenance requirements and can be expected to operate efficiently in excess of 20 years [4, 5].

The technology is currently developed to the point that tax breaks are now available for installing a GSHP system in several countries. The United States government passed The Emergency Economic Stabilization Act of 2008 (Public Law 110-343) includes the Energy Improvement and Extensions Act of 2008 offering tax credits for the installation of a GSHP system. The law offers a tax credit equal to, 30% for residential applications and 10% for commercial applications, of the total investment cost.

The Conventional GSHPs heat exchangers are installed in deep boreholes drilled in the earth. Borehole heat exchangers (BHEs) are becoming more common and much research has been conducted since the 1970s on these systems [6]. The main disadvantage to BHE systems is the initial cost to drill deep boreholes needed to meet the heating and cooling load requirements. The initial capital cost is about 30-50% higher than air source heat pumps [7-9].

Geothermal energy pile (GEP) systems can help alleviate the problem of high initial capital costs. GEPs are based on the combination of borehole heat exchangers (BHEs) and deep foundations that provide structural support. GEP systems have been developed more recently and have an increasing demand because of their energy efficiency and economic benefit [10]. Deep foundations were first used for geothermal heat extraction in the 1980s through the use of circulation pipes placed in concrete elements near the ground [11]. Both types of geothermal heat exchangers, GEPs and BHEs are coupled with GSHPs providing a more efficient alternative to conventional air source heat pumps.

The ground works well as a heat exchanger because the underground temperature stays constant throughout the year. The ground temperature below 15m underground is not affected by the seasonal change in outdoor air temperature [12]. Conventional heat pump systems using outdoor air as a heat sink are less efficient than using the ground because of the amount of heat lift required. The heat lift is the temperature difference between the source of thermal energy and the final destination of the energy. During the summer months heat pumps are used for cooling, and the ground temperature will be significantly lower than the outdoor air temperature. Exchanging heat with ground temperature decreases the heat pump lift in comparison with the outdoor air temperature.

The heat lift will also decrease in the winter when the heat pump is used for heating; the ground temperature will be higher than the outside air temperature. Decreasing the heat lift increases the coefficient of performance (COP) of the heat pump. The COP is an efficiency metric defined as the ratio of heating or cooling energy provided compared to the electrical energy put in to the system shown in Equation 1.

$$\mathrm{COP} = \frac{Thermal\ Output}{Electrical\ Input} \tag{1}$$

The average ground temperature around the United States is illustrated in Figure 1. A GSHP uses the average ground temperatures for heat exchange throughout the year.

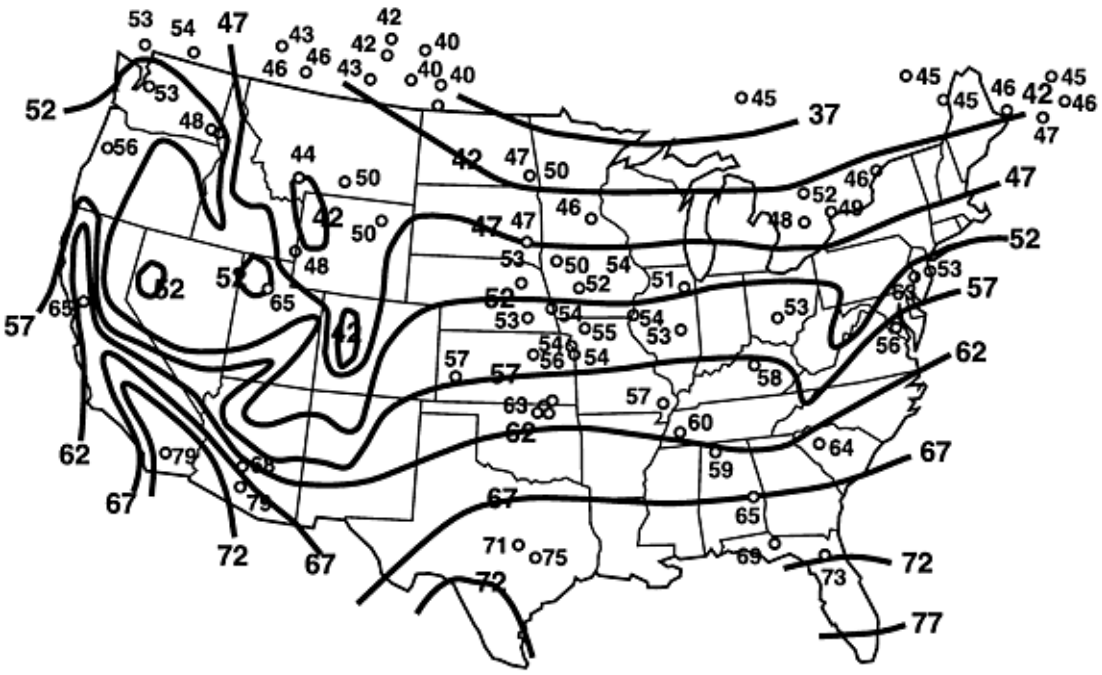

Figure 1: The annual average ground temperatures around the United States [13].

A basic diagram of the heat transfer within a heat pump is shown in Figure 2. The primary loop of a GSHP is the ground loop used to extract or inject heat into the ground in heating and cooling mode respectively. The secondary loop of the heat pump is the loop that interacts with the living space of building or home. The secondary loop of the heat

pump can be used for space heating and cooling or for domestic water heating. When the heat pump is in heating mode the primary loop extracts heat energy from the ground, transfers that heat to the working fluid or refrigerant, inside the heat pump. The working fluid in the heat pump is compressed and then transfers the heat energy to the secondary loop. The process happens in reverse in cooling mode. The secondary loop extracts heat energy and injects it into the ground after being transferred through the heat pump. The working fluid inside the heat pump changes the direction of flow in order to switch between heating and cooling modes.

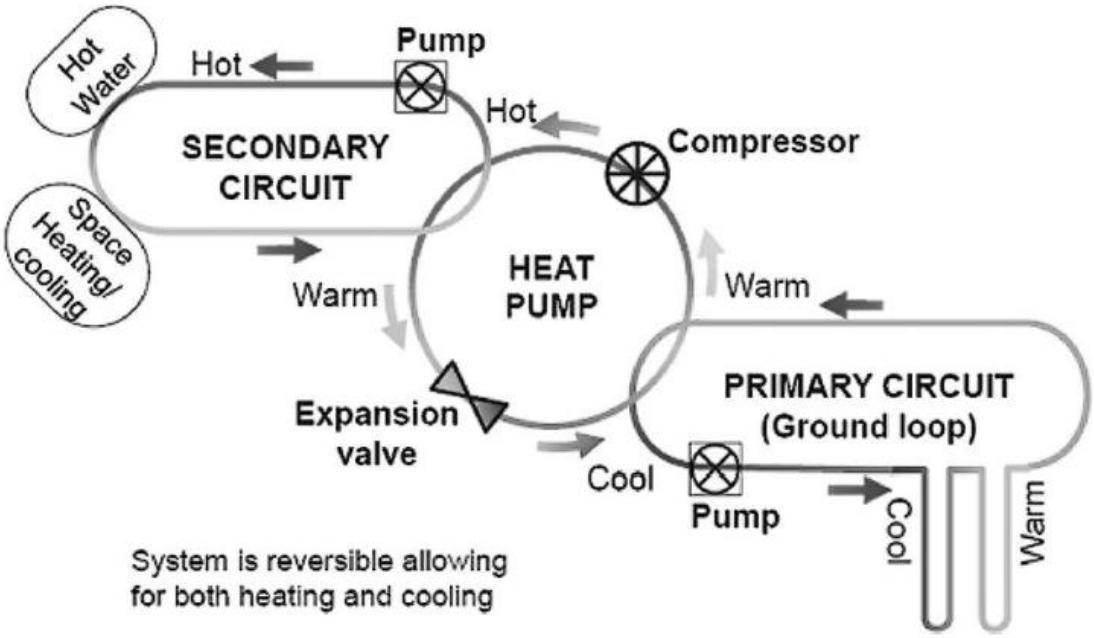

Figure 2: Diagram of reversible heat pump operation, the fluid inside the heat pump loops reverses direction when switched between heating and cooling modes.[10]

Geothermal heat exchangers take advantage of the relatively constant ground temperature to extract or accept heat for use in a GSHP. Various types of geothermal heat exchangers can be coupled with GSHPs. The vertical closed loop design or BHE is the most popular and relevant to this study. GSHP systems use a loop buried underground to

circulate a heat exchange fluid that extracts or injects heat into the ground. High density polyethylene (HDPE) pipe is typically used to contain the heat exchange fluid in a closed loop. Water is the typical heat exchange fluid but sometimes a water/propylene glycol mixture [14] is used to ensure that the fluid in the primary loop does not freeze.

1.2 Borehole Heat Exchangers

The vertical closed loop design, BHE, is the most popular design and is good for retrofitting existing buildings because of the small land area required with minimal disturbance to existing landscapes. The borehole depth is typically drilled from 75 to 600ft (20 to 200m). Depending on the required load the system may contain one to hundreds of boreholes installed in grids [2]. Typically multiple vertical wells are used either in parallel or series (Figure 3) to meet the heat transfer requirements of the system. Drilling to reach the necessary borehole depth is expensive creating a high installation cost.

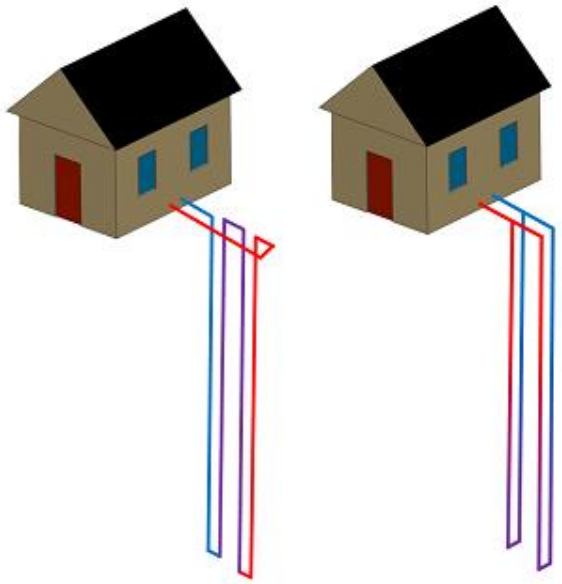

Figure 3: Vertical BHEs, left: two loops in series, right: two loops in parallel.

Vertical systems have low pumping requirements and use the least land area of closed loop systems. Little seasonal variation in ground temperature is experienced

because of the depth of the boreholes [4]. Vertical loops also tend to use less piping per required load because the ground temperature at greater depths is less affected by ambient conditions [15]. When installing a BHE, deep small diameter holes are drilled and the HDPE pipes are inserted into the borehole. The HDPE pipes are referred to as loops or U-loops because of the U-bend that each pair of pipes makes at the bottom of the borehole. One or two loops can be installed in a single BHE. The borehole is then backfilled typically with a thermally enhanced bentonite grout.

1.3 Energy Piles

Large amounts of energy can be saved and long term heating and air conditioning costs can be significantly lowered if more consumers adopt GSHPs for their homes and businesses. The largest reason GSHPs are not more widely used is the initial capital cost of installation to consumers who might otherwise use this sustainable technology. GEP systems help alleviate the problem of a high initial capital cost. GEPs are a combination of a buildings geothermal heat exchangers and deep earth structural foundations. Combining these two systems effectively negates the additional cost of drilling boreholes for a GSHP. Structural piles must be installed to meet the structural requirements of the building, regardless of what type of heating and cooling systems used within the building. The same heat pumps can be used while the length of loop and other components are similar between the two systems, Brandl [16], Martin et al. [17]. The key factor in the sustainability of a GEP system is utilizing geo-structures that are already needed for structural purposes [18]. In addition to offsetting the initial installation cost, concrete has a high thermal conductivity (TC) and thermal storage capacity making it good for use as a heat exchanger and energy absorber, Brandl [16].

Foundations slabs were the first structural elements of a building to be used for heat transfer with the ground. Precast driven piles and later bored piles and diaphragm walls were all successfully developed to be used with heating and cooling purposes, Adam [11]. Prefabricated driven piles represented the majority of energy piles for many years but since the year 2000 large diameter bored piles have been steadily increasing [16]. Figure 4 shows a steel reinforcement cage with heat exchanger loops attached and ready to be inserted into a large diameter bored pile such as the ones studies later in this paper.

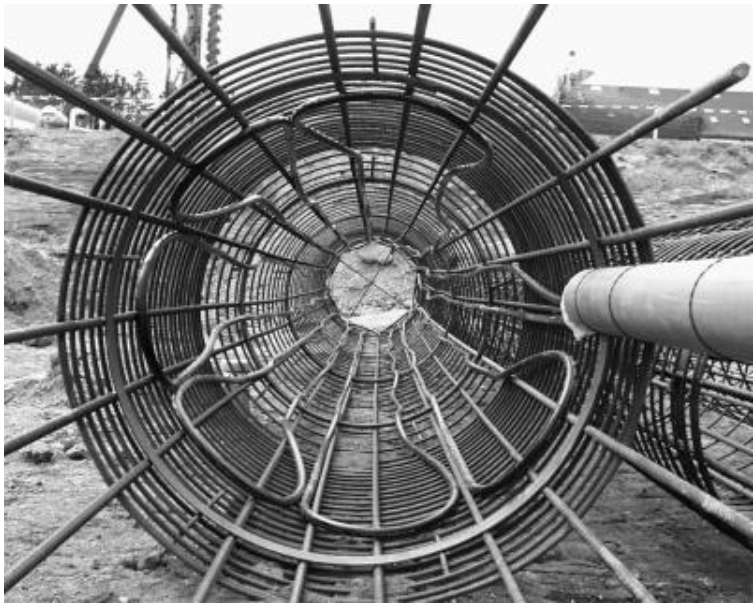

Figure 4: loops inside of a large diameter bored pile steel reinforcement cage.

A similar reinforcement cage with attached heat exchanger loops, is shown in Figure 5 inserted into the casing of a large diameter auger pile with the auger in the background. The GEP system studied in Chapter 2 of this paper falls in the large diameter bored pile category, an Auger Pressure Grouted Energy (APGE) Pile^{TM}. Large diameter piles can be constructed with a casing that allows the reinforcement cage to be inserted before the concrete is poured or the reinforcement cage can be inserted into the liquid concrete after it has been poured.

The HDPE pipes used in GEP systems are typically pressurized before being inserted into the filled concrete pile or before the concrete is pumped in to ensure that loops do not become damaged and the flow is unrestricted. The pressurization of the loops also serves as an integrity check before the loops are closed [16]

APGE piles are Auger Pressure Grouted (APG) piles, first developed in the 1940s, with the addition of HDPE pipes for coupling with a GSHP. APG piles are also known as auger cast and continuous flight auger piles. The Deep Foundations Institute has since established the generic term of Augured Cast-In-Place piles.

Figure 5: large diameter auger pile with reinforcement cage and heat exchanger loops inserted, the auger is in the background.

APGE piles are installed by rotating a hollow stem continuous flight auger into the ground until the desired final depth of the pile is reached. High strength fluid grout is then pumped under pressure out of the auger tip. A predefined amount of grout is pumped out until a sufficient pressure head is developed. The auger is then withdrawn in a slow and controlled manner while rotating and maintaining the pressure head to ensure the structural integrity of the pile is not compromised by intrusion of foreign material or vacancies in the pile. The loops similar to the experimental pile simulated in Chapter 2 can be seen in Figure 6. The loops and center steel support are inserted into the grout after the column is withdrawn. [19, 20]

Figure 6: The loops used in the experimental piles from the Berkel test site.

The loops are attached to a 1inch (25mm) diameter steel center rod extending to the full length of the pile. The center of the HDPE pipes are approximately 3inches (7.6cm) from the center bar. The center of the two legs of each loop are approximately 3inches (7.6cm) spread apart from each other. [19, 20]

1.4 Thermal Response Test

To properly design a GSHP system it is essential to know the thermal properties of the local soil and rock formations. High confidence in the ground thermal properties leads to improved design and possibly results in significant financial savings by decreasing overdesign [21]. A thermal response test (TRT), also known as a thermal conductivity test, is an in-situ test method for determining the local thermal properties of the soil.

The TRT was first presented by Mogensen [22] in 1983 as an in situ method to determine the values for the thermal conductivity and thermal resistance. Mogensen suggested using a water chiller to circulate chilled water at a constant cooling rate and measuring the temperature response. Mobile TRT devices (Figure 7) were developed for the first time in 1995 when devices were made in both Sweden and the USA [12]. The device being developed in the USA was developed at Oklahoma State University [23]. The Swedish device was developed at Luleå University of Technology [24, 25]. Both the Swedish and American device operated on Mogensen's principles but used a heater instead of a chiller to inject a heat rate into the ground [12].

The knowledge of the local thermal properties is of great importance in the design of GSHP systems. The TRT estimates these properties by testing an installed geothermal heat exchanger similar to those that are designed and planned for the site. A heat transfer fluid is circulated through the heat exchanger being tested while applying a constant heat

rate to the fluid. The inlet and outlet temperatures, the flow rate, and heat rate of the test are measured. The results are then compared to a mathematical model to characterize the thermal response of the borehole[26].

Mobile TRT test rigs are enclosed in a sealed cabinet and insulated, the above ground pipes and tanks are insulated to reduce heat loss and ambient effects [26]. Generally temperature sensors are mounted inside the test unit but ambient effects can be mitigated also by installing temperature sensors in the borehole or pile itself [21].

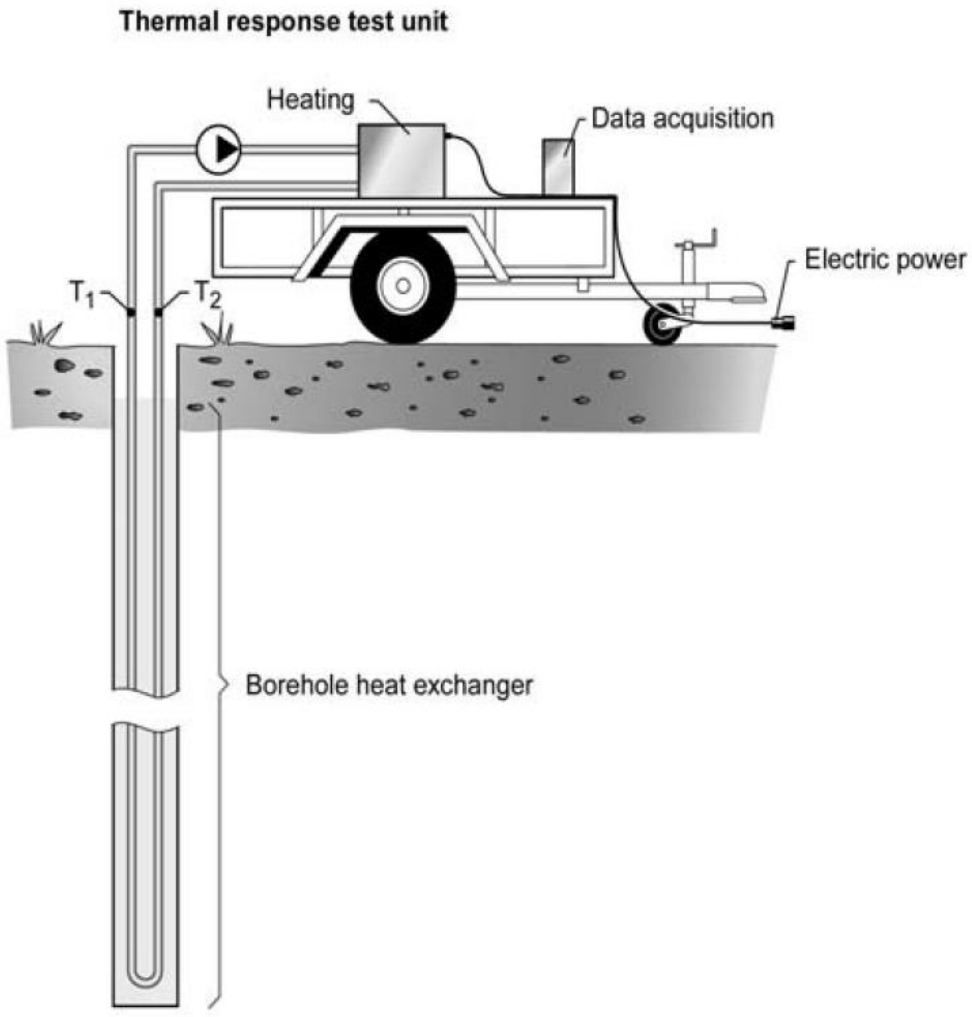

Figure 7: A basic concept of a mobile TRT setup, Gehlin (2002).

The TRT produces an overall effective TC value for the geothermal heat exchanger taking into account all of the soil conditions and underground formations. The test will not provide information about the thermal characteristics of different soil layers or formations underground. TRTs tests are commonly practiced in the USA and have been standardized by the American Society of Heating Refrigeration and Air Conditioning Engineers (ASHRAE) explained by Kavanaugh, 2001 [26].

1.4.1 Testing with Boreholes vs. Energy Piles

Testing guidelines and standards for BHEs are available from three different sources, the American Society of Heating Refrigerating and Air Conditioning Engineers (ASHRAE) [26], the International Energy Agency (IEA) [27] and the Ground Source Heat Pump Association in the UK (GSHPA)[28],[10]. The industry has become well acquainted with conducting TRTs on BHEs and very specific guidelines for how they are to be completed have been developed. Some of the important guidelines pertaining to BHEs recommended by ASHRAE presented by Kavanaugh [26] are listed below.

- TRTs test duration should be 36 to 48 hours
- The applied heat rate should be 15 to 25 W/ft (50 to 80 W/m).
- Data collection should be at least every ten minutes
- The minimum measurements to record should be the temperature at the inlet and outlet of the borehole, the initial ground temperature, input power to the heating elements, and the ground heat exchanger depth.
- A period of twelve days is required before a retest can be done if a full 48 hours of testing has been completed

- A waiting period of three days for high conductivity and five days for low conductivity is required after installation before the TRT is conducted.
- The initial ground temperature should be measured at the end of the waiting period by direct insertion of a probe or by measuring the temperature as the liquid exits the loop.

Recently the GSHPA published a manual on the design and construction of GEP systems, including TRT guidelines for GEPs. Testing guidelines and standards for GEP systems are not as well developed as BHEs. The diameter of an energy pile is significantly larger and the depth is typically much less. Testing methods for BHE systems assume a high length to diameter ratio so that the shape of the borehole approaches a line [10]. The difference in geometry means that the testing practices of BHEs do not necessarily apply to GEPs. The GSHPA association has made the following recommendations in regards to conducting TRTs for GEP systems [29].

1. When the potential use of GEP systems is identified early in the design process a BHE can be constructed with a single loop and tested to find the local thermal properties.
2. If the designed piles are no larger than 30cm in diameter than a TRT can be carried out using the recommendations made for a BHE system.
3. If the GEP system design consists of piles larger than 30cm then a TRT of longer duration and involving more sophisticated interpretation techniques can be done.

4. One of the testing options above could be extended to incorporate a stress strain analysis as well as a thermal analysis in order to better understand the structural and thermal behavior of the pile under a thermal load.

In regards to option 3, the test duration should be extended to ensure that the thermal resistance of the pile is overcome. The test time should be extended based on Equation 2, where it is generally considered that times less than t_1 should be discarded when using line source interpretations.

$$t = \frac{5\, r_o^2}{\alpha} \tag{2}$$

The extended testing time ensures that the pile thermal resistance has reached a near steady state behavior. Comparing the test results to a different method besides the line source method could reduce the testing time. To conduct a complete load test as described in option 4 the pile has to be fully instrumented with strain gauges and temperature gauges. A full instrumentation would provide the most realistic data but is not as economically feasible for smaller applications. [29]

1.5 Line Source Method

The line source method is an analytical solution that solves for the temperature distribution around geothermal heat exchangers. The line source method is commonly used to approximate temperature distributions around BHEs and GEPs and is a useful comparison tool. Ingersoll and Plass found that if you treat the geothermal heat exchanger as a constant infinitely long line source of heat in an infinite medium with a uniform initial temperature then the temperature distribution is given by Equation 3 [30].

$$\Delta T(t) = -\frac{q}{4\pi k H} Ei\left(\frac{r^2}{4\alpha t}\right) \tag{3}$$

The infinite line source method was developed by integrating Kelvins point source in an infinite medium along a line of infinite length. This approach does not account for any end effects of the heat source. An approximation of the line source theory (Equation 4) was developed by Carslaw and Jaeger[31].

$$\Delta T = \frac{q}{4\pi kH} ln \frac{4\alpha t}{r^2} - \frac{\gamma q}{4\pi kH} \tag{4}$$

The line source is widely used when solving the temperature distribution of BHE systems. The high length to diameter aspect ratios make the geometry similar to a line. The line source method is less suitable for GEP systems with lower length to diameter aspect ratios and shaped less like lines. Zeng et al. [32] developed a finite line source method (Equation 5) accounting for the end effects of the heat exchanger by using a virtual sink with an opposing heat rate to ensure that the ground temperature remains constant.

$$\Delta T = \frac{q}{4\pi k} \int_0^H \left[\frac{erfc\left(\frac{\sqrt{r^2 + (z-h)^2}}{2\sqrt{\alpha t}}\right)}{\sqrt{r^2 + (z-h)^2}} - \frac{erfc\left(\frac{\sqrt{r^2 + (z+h)^2}}{2\sqrt{\alpha t}}\right)}{\sqrt{r^2 + (z+h)^2}} \right] dh \tag{5}$$

The behavior of the heat exchanger will eventually approach the behavior of a line heat source with a constant heat rate. The line source method assumes the soil is a uniform and isotropic medium. The temperature difference between the inlet and outlet of the system is assumed to remain constant through time. This method is inaccurate for first few hours of the test so experimental data from the beginning of the test must be ignored. The line source method is often used to simulate long term heating or cooling loads with unbalanced seasonal heat injection and extraction. An imbalanced system will thus result in a long term temperature change of the local soil that could take a number of years to reach a steady value.

1.6 Heat Transfer Mechanisms

The heat transfer mechanisms that take place in BHEs and GEPs are relatively simple and well understood concepts. Conduction and Convection are the two primary heat transfer mechanisms. Conduction is the transfer of energy from more energetic particles to less energetic particles as a result of their interaction. The rate of conduction heat transfer can be quantified by Fourier's Law (Equation 6), the heat rate per unit area or heat flux is proportional to the change in temperature divided by the distance between the two temperatures. The thermal conductivity "*k*" is the proportionality constant of the respective material with units of W/m·K.

$$q'' = \frac{q}{A} = k\frac{\Delta T}{\Delta x} \tag{6}$$

Convection is the transfer of energy through the conduction of a fluid and the fluid's bulk motion. Convection is defined by Newton's Law of Cooling (Equation 7). The heat transfer is enhanced by the bulk motion of the fluid as large quantities of particles move together.

$$q'' = \frac{q}{A} = h \cdot \Delta T \tag{7}$$

The convection heat transfer coefficient "*h*" is the proportionality constant having units of $W/m^2 \cdot K$.

Convection and Conduction are the heat transfer mechanisms occurring between the fluid and the HDPE pipe wall as the circulation fluid flows through the geothermal heat exchanger. Conduction is occurring between the HDPE pipe, the pile, and the surrounding soil transferring heat away from the geothermal heat exchanger. The heat diffusion equation (Equation 8) defines transient conduction

$$\frac{\partial T^2}{\partial x^2} = \frac{1}{\alpha}\frac{\partial T}{\partial t} \tag{8}$$

The heat diffusion equation will provide the temperature distribution as a function of time. These heat transfer concepts are the foundation of the complex heat transfer taking place inside a geothermal heat exchanger. The moisture of the soil also has a significant effect on the heat transfer but is dependent on the local ground conditions. [33, 34]

The thermal resistance of a system is a measure of the temperature difference between two locations in the system. The general equation for thermal resistance is shown in Equation 9. The thermal resistance can be categorized as the ratio of a driving potential to the corresponding heat transfer rate.

$$R = \frac{\Delta T}{Q} \tag{9}$$

In regards to energy piles the thermal resistance is an important metric used to describe how effectively the pile geometry transfers heat to the surrounding soil. The thermal resistance can be used to make comparisons between different pile geometries.

1.7 Geothermal Energy Pile Performance

Piles and boreholes are analyzed on their performance using several different metrics. The thermal response of the system is important because it can be used to explore the in-situ performance of the pile and used for design purposes. The thermal response is measured as a function of time and is the output of a TRT. These tests and responses are almost always needed to aid in the design of a system.

The rate of heat transfer in the system or calorimetric power measured in Watts is of great interest as well [10]. The temperature difference between the inlet and outlet can also be used to measure the amount of heat transfer happening within the system as is the

case for TRTs. The calorimetric power measures the amount of heat that is transferred in the geothermal heat exchanger and can be measured as a function of the heat flux leaving the fluid in a numerical simulation.

The pile thermal resistance is another important metric used to measure the performance of a GEP. The pile thermal resistance is important to the design of geothermal energy piles because it is a measure of the temperature gradient between the fluid and the outer wall or surface of the pile. Reducing the temperature gradient across the pile is important when making design decisions for geothermal heat exchanger systems. This can be accomplished by ensuring that the flow is turbulent, using higher thermal conductivity materials and increasing the number of loops in a pile. The borehole resistance of vertical geothermal heat exchangers is calculated based on Equation 10 [10, 35].

$$T_f = T_{pw} + \frac{q}{H} R_p \tag{10}$$

The temperature of the fluid and the pile surface is commonly assumed to be constant for the entire pile. This is truer in some cases than others the mean values can also be used to calculate the resistance.

1.8 Computational Fluid Dynamics Model Physics

ANSYS 13.0 CFX is the computational fluid dynamics (CFD) software that was used to perform the numerical simulations in this paper. ANSYS 13.0 CFX solves the unsteady Navier-Stokes equations in the conversation form. The Navier-Stokes equations are commonly referred to as the governing equations. The governing equations are broken down into the continuity equation, the momentum equations and the energy equation. Each of these has a conservation and nonconservation form. The conservation forms of the equations used by ANSYS are the specific integral forms of the equations obtained when

analyzing a control volume that is fixed in space. In contrast the nonconservation forms of the equations are obtained from a flow model with the control volume moving with the flow [36]. ANSYS 13.0 CFX solves the conservation form of the governing equations. The governing equations used in the simulation are given in the ANSYS CFX Solver Theory Guide[37]. The continuity equation (Equation 11) governs the conservation of mass in the CFD simulation.

$$\frac{\partial \rho}{\partial t} + \nabla \cdot (\rho U) = 0 \tag{11}$$

The conservation of momentum equation are shown in Equation 12. The conservation of momentum equations maintain that Newton's second law stay true, any forces acting on a body must equal that bodies mass times acceleration.

$$\frac{\partial (\rho U)}{\partial t} + \nabla \cdot (\rho U \otimes U) = -\nabla p + \nabla \cdot \tau + S_M \tag{12}$$

Where the stress tensor, τ, is related to the strain rate by

$$\tau = \mu \left(\nabla U + (\nabla U)^T - \frac{2}{3} \delta \nabla \cdot U \right)$$

For conservation of energy the thermal energy equation was chosen over the total energy option. The total energy equation can be used for high speed flows with high density variance while the thermal energy equations are suitable for low speed flows. The thermal energy option (Equation 13) works well for liquids where variable density effects are negligible. The variable density effects of water are neglected in this analysis and properties of water are constant throughout this investigation.

$$\frac{\partial (\rho e)}{\partial t} + \nabla \cdot (\rho U e) = \nabla \cdot (\lambda \nabla T) - p \nabla U + \tau : \nabla U + S_E \tag{13}$$

The Reynolds number of the flow in Chapter 2 of this paper was known to be approximately 26,000 based on the experimental data and 6,200 in the Chapter 3 analysis based on the geometry and boundary conditions. Turbulent flow through a circular pipe is known to begin developing turbulence when the Reynolds number reaches approximately 2,300 [33]. The calculated Reynolds number confirms the flow is turbulent inside the HDPE pipes and therefore a turbulence model is needed within the CFD solver. The k-epsilon turbulence model was used and is a two equation turbulence model. The two added equations solve for k, the turbulence kinetic energy and ε, the turbulence eddy dissipation. The k-epsilon model is more generally an eddy viscosity turbulence model based on the principle that turbulence is made up of small eddies that are always forming and dissipating within the flow causing Reynolds stresses proportional to mean velocity gradients. The k-epsilon model was chosen because it is a commonly used turbulence model that provides a good balance of numerical effort and computational accuracy. When tested alongside the other turbulence models the k-epsilon model produced good residual convergence results and relatively fast computation times. The turbulence models are explained in detail in the ANSYS CFX Solver Theory Guide [8].

Chapter 2: Numerical Modelling

The ANSYS 13.0 CFX model discretizes all physical domains that exist in the original experimental setup including the fluid domain, incorporating CFD analysis into the model. Using CFD to model the energy pile increases the ability to monitor characteristics of the fluid thermal behavior and flow characteristics. Using the CFD model a field test was modeled as it was conducted in the field; with the input heat was introduced to the fluid above ground and the fluid dissipated the heat to the surrounding soil through the loops.

2.1 Experimental Test Program

The experimental testing program was operated by Berkel and Company Contractors Inc. at their Richmond, TX regional office. Three GEPs were constructed and instrumented at the test site for GEP research. The test site consists of three GEPs that were tested individually and as a group. Each of the three piles use 1inch (25mm) loops installed to the full depth of the piles. Two of the piles were installed with a structural pile grout mix, one 30cm diameter pile and one 45cm diameter pile. The structural grout results in a compressive strength of 4,000psi (27.5 MN/m^2) in 28 days. The third pile was 30cm and constructed with a thermally enhanced bentonite/silica grout typical of a BHE. The experimental test setup and GEP configurations are discussed by Brettmann [20]. The layout of the three piles and the onsite soil boring can be seen in Figure 8. The soil boring revealed alternating layers of clay and sand with the first layer being clay down to a depth of 10m.

Figure 8: The layout of the experimental test site including the three piles and soil boring locations.

The ground water table (GWT) was located in the first layer of clay at a depth of 3.3m. The next layer of soil was sand from 10 to 17m. The third layer of soil was a relatively thin 1.5m layer of clay and then the fourth layer was sand extending to the final depth of the boring 21m. Samples from the boring and grout underwent thermal conductivity tests in accordance with the ASTM D5334 testing procedures [38], the results from the laboratory tests are displayed in Table 1.

Table 1: laboratory soil TC test results [19]

Sample	*Moisture Content (%)*	*Dry Weight (pcf)/(Mg/m^3)*	*TC (Btu/hr*ft*F)/(W/m*K)*
Clay - 20ft (6.1m)	21.1	107.7 / 1.73	1.28 / 2.22
Sand -45ft (13.7m)	14	108.6 / 1.74	2.34 / 4.05
Clay - 60ft (18.3m)	28	96.3 / 1.54	1.21 / 2.09
Thermal Grout	64.5	57.8 / 0.93	0.78 / 1.35
APGE Pile Grout	7.3	118.9 / 1.91	0.78 / 1.35

The TRTs were conducted using the equipment in Figure 9. This test setup is used to heat the fluid with a near constant heat rate. The heat rate recorded experimentally from this unit fluctuated ±5%.

Figure 9: The TRT Test Unit used at the experimental test site.

The mobile unit was insulated to minimize ambient effects on the test results. Inside the insulated mobile test unit is a heater, a control unit, a pump and temperature sensors to measure the inlet and outlet flow temperature.

2.2 Experimental Validation of the CFD model

The CFD model discussed in this chapter simulates the double loop test conducted on the 30cm APGE Pile^{TM} with standard structural grout [20]. Using CFD to simulate the GEP provides an advantage over other methods because the fluid domain is discretized improving the analysis of the heat transfer within the pile. The fluid flow and heat transfer details of fluid are modeled providing additional insight compared to models that are simplified to exclude their discretization.

2.2.1 Model Geometry

The 30cm pile geometry was modeled as it was constructed. It consists of two loops joined at the top for operation in series. The model inlet is above the top of the soil domain, the fluid enters immediately into a heated length where the simulated TRT heat rate is applied to the fluid before entering the first loop in the pile. The fluid then flows through the two loops connected in series by a U-shaped connector above the pile's upper surface and flows to the outlet. The entire model can be seen in Figure 10 with the top and bottom of the pile geometry enlarged. The top of the pile is enlarged to highlight the model inlet, outlet, heated length and the U-shaped connector that connects the two loops. The soil domains are thick cylindrical domains around the 30cm pile. Total height of the soil domains is 25m and the diameter of the domains is 20m. Brettman [20] found that the initial soil temperature does not change more than 2.6m from the pile. The pile is

18.3m deep, the center loops extend to the bottom of the pile. The outer diameter of the HDPE pipes is 3.34cm and the thickness of the pipe is 3mm. The fluid domain has 2.73cm diameter equal to that of the inner diameter of the HDPE pipe. The heated length of the fluid domain is 1m long where the fluid enters through the model inlet and then curves down into the HDPE pipe. The heated length of the fluid is not surrounded by an HDPE pipe domain because the heat rate is applied directly to the fluid along this heated length.

Unlike similar numerical models the CFD model discretizes the HDPE domain and the fluid domain in addition to the pile and soil domains. The fluid domain is blue and the HDPE pipe is grey in Figure 10. The fluid domain and the HDPE pipe domain are modeled as they are in the experimental setup. The model consists of eight domains representative of the experimental test pile, the fluid domain, the HDPE pipe, the 30cm pile, and the five soil layers. To simplify the model the steel support and the rubber spacers were not discretized in the model and were considered insignificant to the heat transfer.

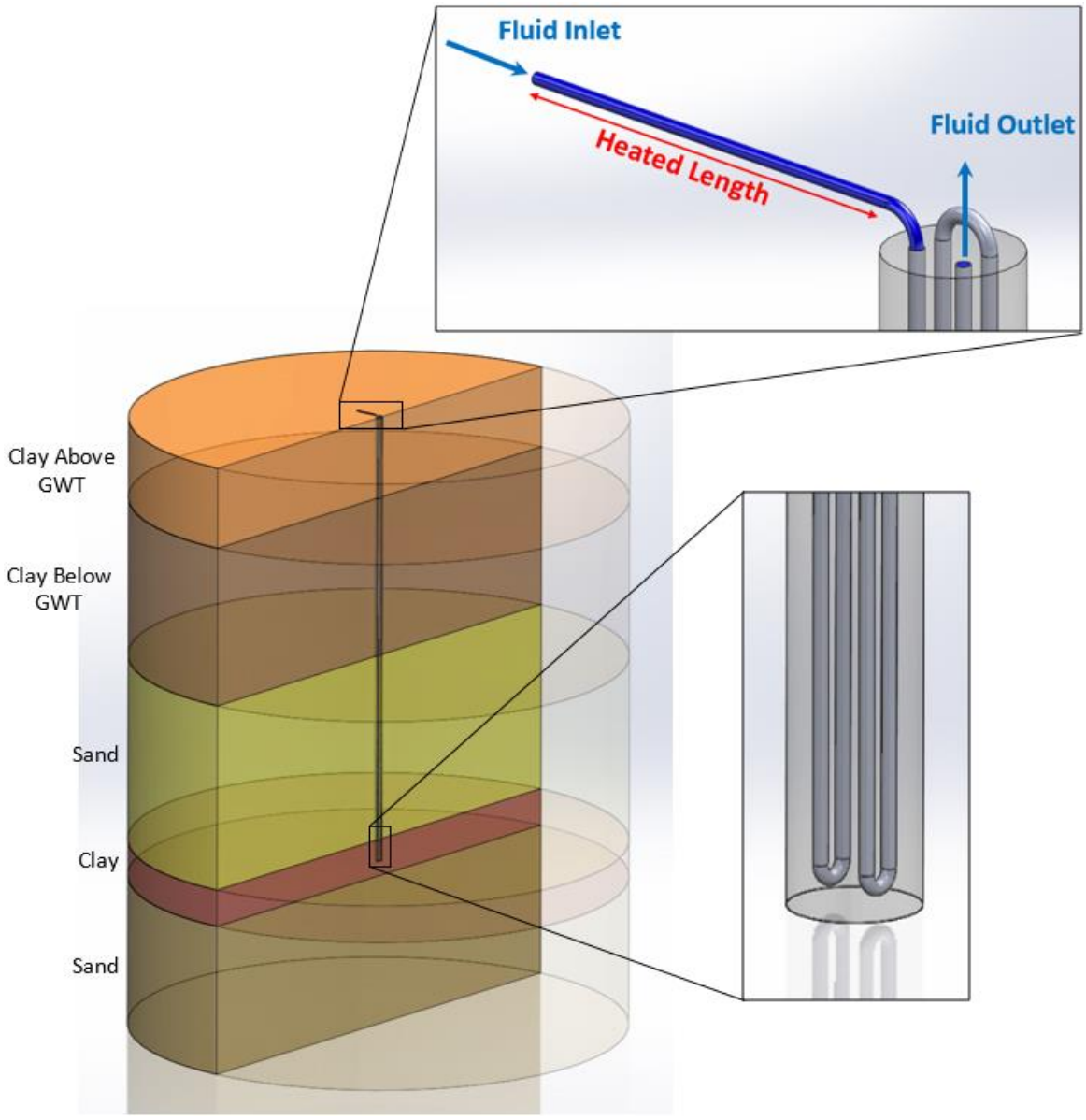

Figure 10: The 30cm pile model with enlargements around the top and bottom of the pile.

The properties of each of the domains in the CFD model are outlined in Table 2 and are sorted by their respective depth in the model. These values were chosen based off of the numerical model constructed by Ozudogru [39] using COMSOL multiphysics [40].

Table 2 : Model Properties of the 30cm pile CFD model

Domain	*Depth [m]*	*Density ρ [kg/m^3]*	*Thermal Conductivity k [W/m·K]*	*Heat Capacity C_P [J/kg·K]*
Clay 1 Above GWT	0 - 3.3	1750	1.7	950
Clay 1 Below GWT	3.3 - 9.8	2095	2.22	1019
Sand 1	9.8 - 17.4	1984	4.05	898
Clay 2	17.4 - 18.9	1971	2.09	1110
Sand 2	18.9 - 25.0	1984	4.05	898
30cm Pile	0.0 - 18.3	2049	1.35	909
HDPE Tube	0.0 - 18.3	950	0.45	2250
Water	0.0 - 18.3	997	0.6069	4181.7

2.2.2 Mesh

The mesh for the energy pile was created using the ANSYS meshing software [41]. The meshing techniques used were primarily focused on keeping the number of cells to a minimum while ensuring that the heat transfer in and around the fluid domain would be resolved.

The soil domains and the 30cm pile were meshed using a hex-dominant method to reduce the number of cells in these domains. The soil domain is large enough that the heat transfer effects should do not extend to the outer walls of the domain [19, 39]. The cells in the pile domain were also meshed with a hex-dominant method and the maximum size of the cells was constrained to 3cm. The maximum size of the cells is constrained in order to ensure sufficient accuracy of the numerical results.

The fluid domain uses a cell inflation on the interior of the pipe wall to help resolve the boundary layers within the fluid flow. Discretization of these domains provides additional heat transfer information about the fluid flow within the system. The detailed

flow characteristics such as the boundary layers on the inside of the pipe wall were not captured in full detail by the mesh because of the large number of cells that would have been required to do so. A high resolution of these features was sacrificed to save computation time and because the flow characteristics are relatively simple. The mesh was severely concentrated inside the pile. The size of the individual mesh elements varied greatly in this model because of the large variation in domain sizes. The HDPE pipe wall is 3mm thick while the soil domain diameter is 20m. The size variation of the domains provided challenges keeping the cell count of the mesh low. The model residual convergence criteria was set to $1x10^{-5}$. The CFD model mesh is displayed in Figure 11 with the five soil domains, the top of the pile, and the bottom of the loops. The mesh concentration inside and around the pile can be seen in the image of the soil domains.

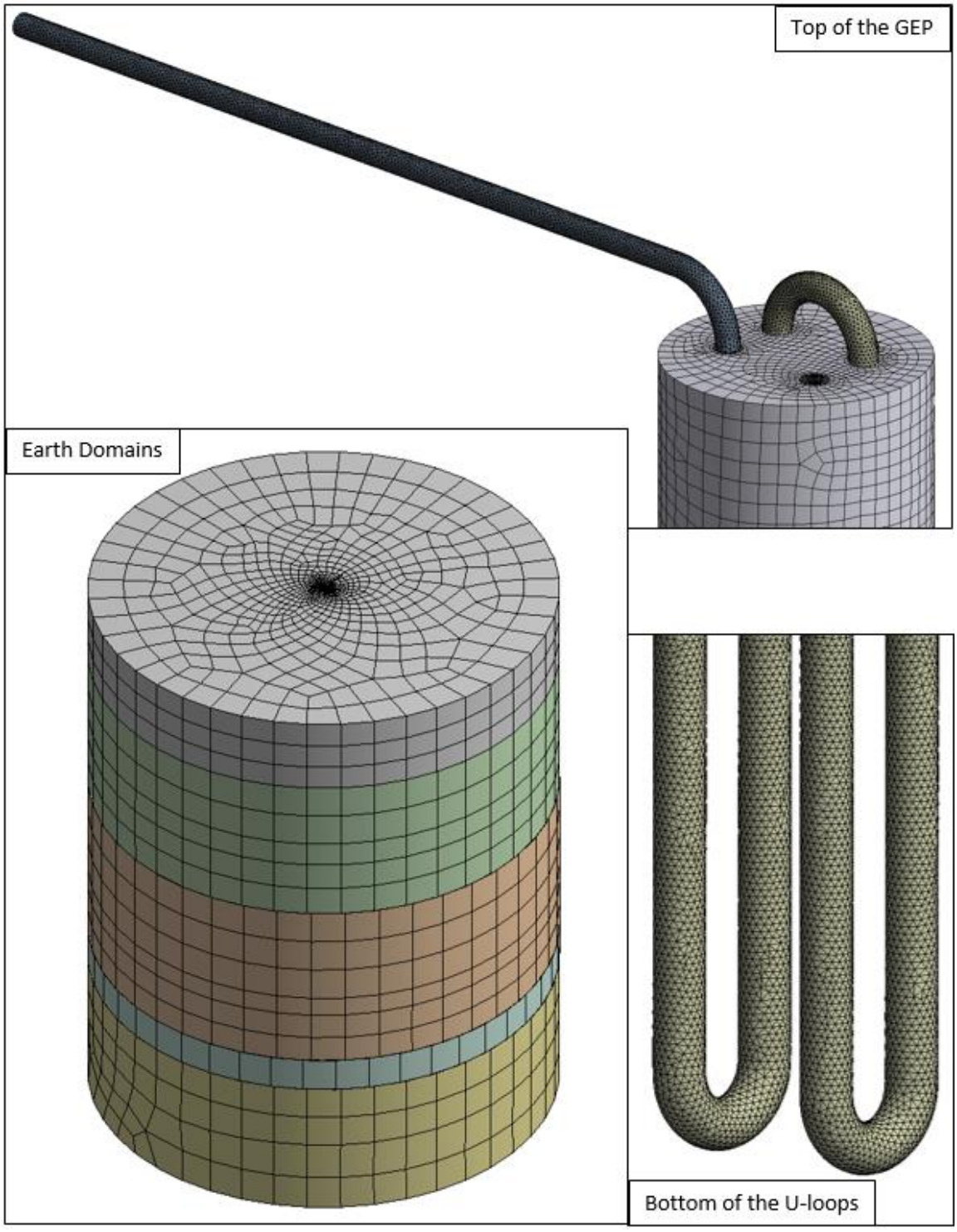

Figure 11: The five soil domains and zoomed views of the top of the pile and bottom of the loops

2.2.3 Boundary Conditions

The CFD model was set up with initial conditions and boundary conditions matching the experimental setup described by Brettman et al. [19, 20]. The initial temperature condition of all solid domains in the model was 22℃ while the initial temperature of the fluid domain was 25.5℃. The fluid and solid domains have different initial temperatures because at the beginning of the experiment, before circulation began, the fluid was at a higher temperature than the ground. The fluid was circulated through the energy pile loops for approximately 20 minutes until the average fluid temperature lowered to 25.5℃, the heater was then turned on beginning the test. The surfaces of all the solid domains at or above ground level had an adiabatic boundary condition imposed on them. The adiabatic condition was imposed on the ground level surfaces of the top soil domain, the pile, the exposed ends of the HDPE pipes, and the loop U-connector that is above ground. The adiabatic ground level condition was imposed because this model did not simulate the effects of the ambient air temperature or solar heat gain effects. The boundary condition of the model's outer walls was a fixed temperature condition simulating the earth as an infinite heat sink. The temperature of the outer wall and bottom wall of the model were fixed at 22℃ and held constant for the entire 96 hours of the transient simulation.

The flow conditions within the energy pile model were set up to model the heat transfer and thermal behavior of the flow as closely as possible. The inlet flow rate was set to a constant 33.7 l/min as reported with the experimental data. The outlet flow pressure was constrained to a static pressure of zero Pa. The pressure constraint on the outlet flow creates the highest measured pressure at the model inlet equal to the total pressure loss in the system. The outlet flow temperature was left unconstrained. The flow was modeled with a no-slip wall condition at the pipe walls, holding the near wall velocity to zero.

2.2.4 Temperature Input Boundary Conditions

The CFD model was first tested using the experimental inlet temperature data as the input to the system. This first iteration of the model had no heat rate boundary condition applied, instead it used the experimental inlet temperature data to govern the thermal response. Using the temperature as the input tests the physics of the model but does not give a validation of the accuracy of the model. The model matched the outlet temperature perfectly when using the experimental inlet temperature as the input to the system. The results of the CFD model using the experimental inlet temperature as the input condition are displayed in Figure 12.

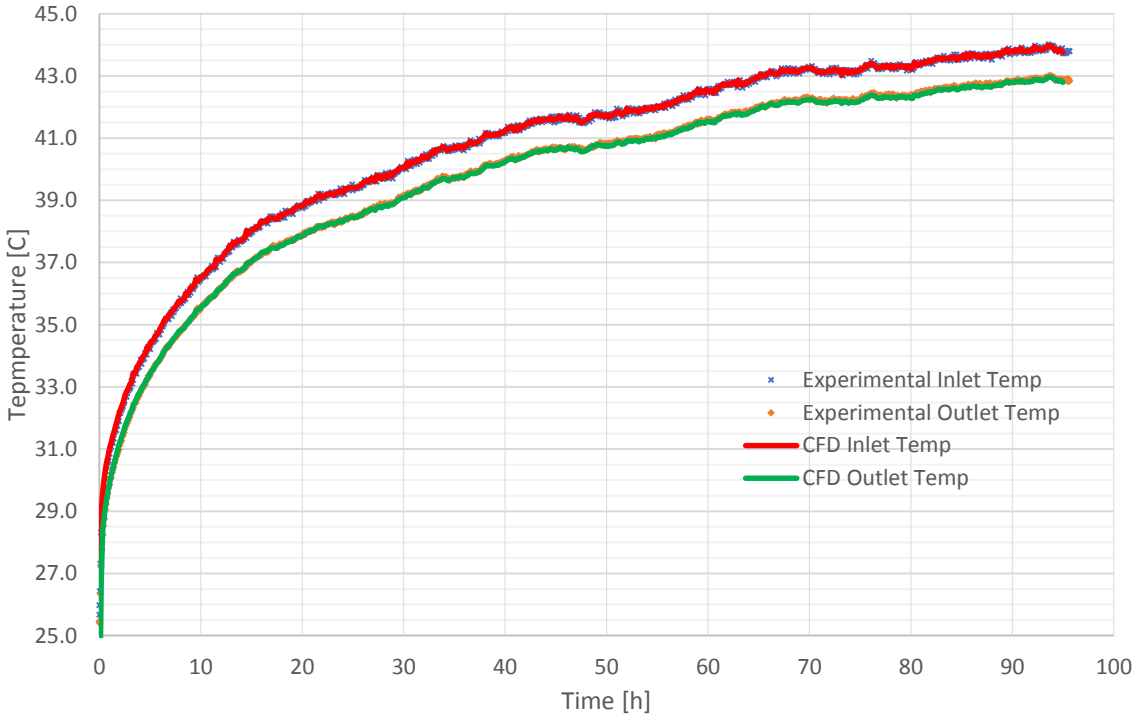

Figure 12: CFD results with the temperature as the input to the system

Setting the model inlet temperature as the input to the system allows the system to calculate the outlet temperature of the flow at each time step but will not propagate the effects of the heat transfer within the pile to the inlet condition of the next time step. If the outlet temperature does not match the experimental data, that result would not be propagated

through the system using these inlet boundary conditions. The heat transfer within the pile had no effect on what the model's inlet temperature would be for the next time step. To validate that the model will accurately reproduce the experimental results, the model had to use the same input to the system as the experimental setup did, the heat rate that was imposed on the fluid.

2.2.5 Heat Rate Input Boundary Conditions

The model was further developed to validate that the CFD analysis could accurately reproduce the experimental results using the true input to the system. The temperature at the beginning of the heated length, the models inlet temperature boundary condition, was set equal to the average outlet temperature at each time step. The outlet flow temperature boundary condition was left unconstrained. Setting the model's inlet condition equal to the outlet condition simulates a recirculating flow through the loops. The transient simulation required that the time steps be sufficiently small for the model to accurately reproduce the field test. The time step size was initially tested at an average of eight minutes and four minutes. The simulations were run for 30 hours and there was no observable difference in the temperature values. The average temperature of the earth inlet and outlet is shown in Figure 13 for the four minute and eight minute time step cases. This test shows that the reducing the time step will not change the results of the model.

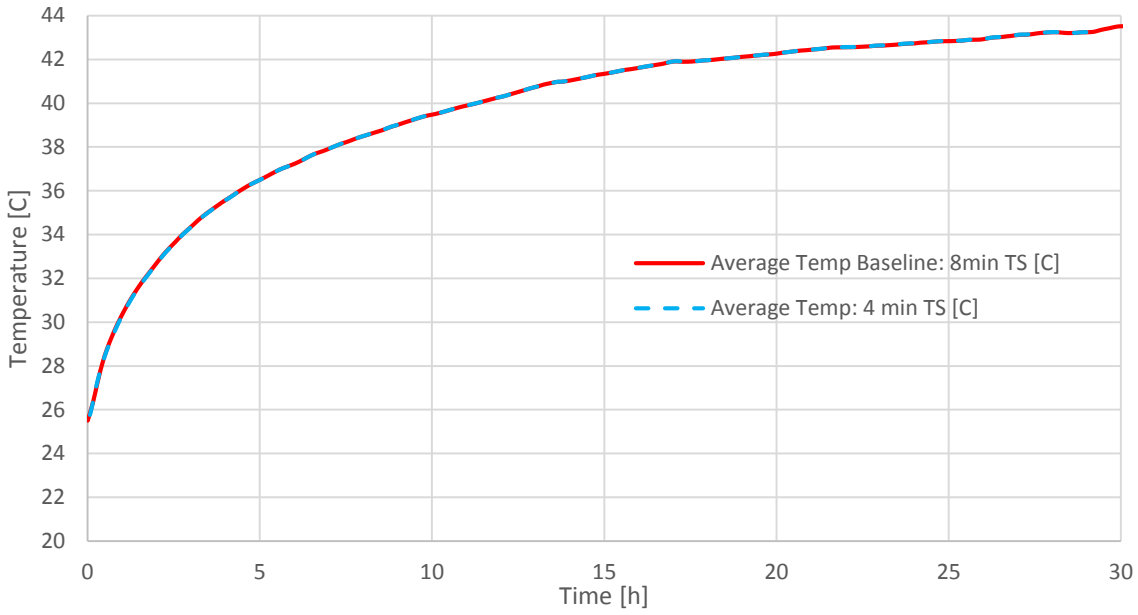

Figure 13: The model was simulated with time steps of 4min and 8min and produced the same results.

The flow characteristics at the outlet, velocity, pressure and turbulence, were not carried over to the model inlet condition because in the physical experimental setup the flow would have to pass through a heater and a pump that would govern the flow conditions at the inlet. The inlet flow rate was held constant through at the field test's recorded flow rate, 33.7 l/min. The heat rate was applied to the fluid as a constant heat flux over the length of fluid labeled "heated length" in Figure 12. The total heat flux applied to that area of fluid was calculated to equal the experimental input heat rate to the system. This heat flux boundary condition inputs the same amount of heat to the fluid as the heater in the experimental setup. The model properties of the baseline case are the values specified in Table 2 and the heat rate is equal to the experimental heat rate. The baseline CFD case results produced a temperature response that was higher than the experimental results. The temperature values from the baseline CFD case were 4℃ above the experimental values. The plot in Figure 14 illustrates the inlet and outlet temperatures for the baseline case and the experimental case. The trend and slope of the temperature response is approximately

the same in the CFD simulation and the experimental data after the initial temperature ramp in the first 20 hours.

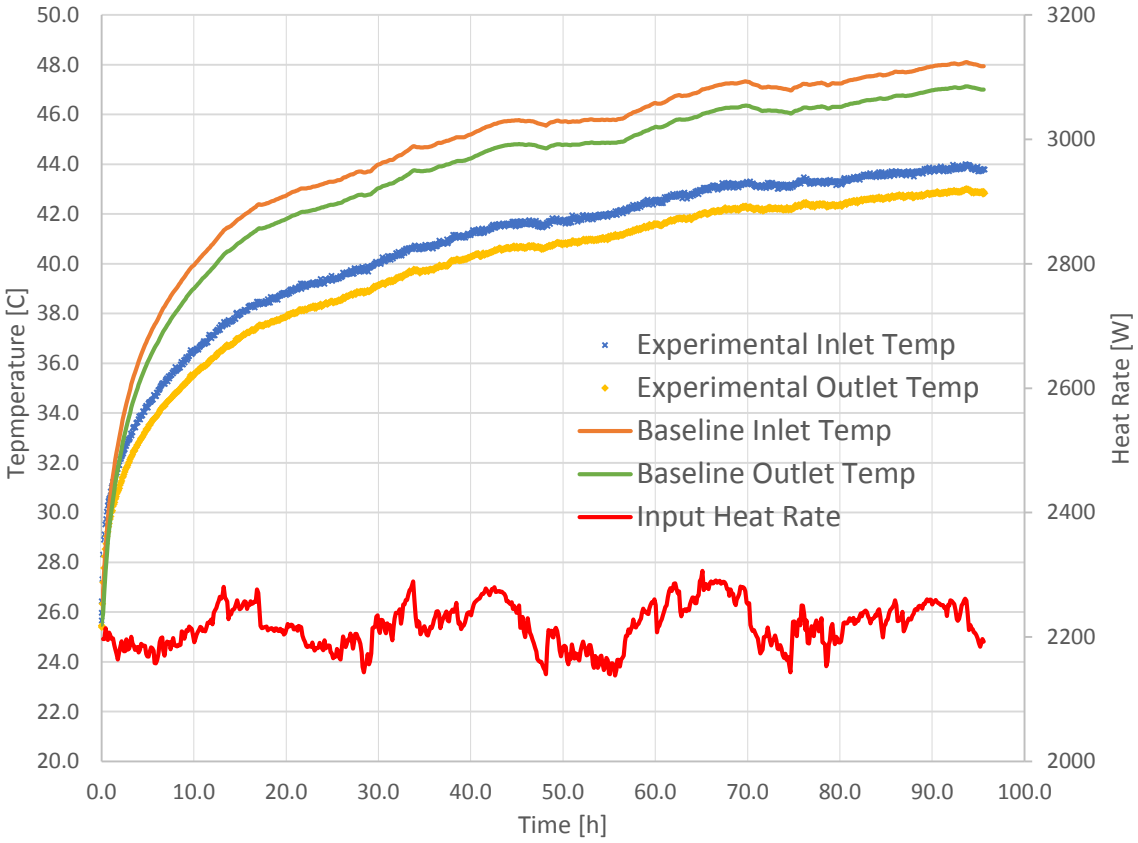

Figure 14: Inlet and outlet temperature responses for the baseline case and the experimental results

The fluctuation in the heat rate was a result of the experimental heater control unit trying to maintain a constant heat rate, the minor fluctuations in heat rate are to be expected when conducting a TRT in the field.

2.2.5 CFD Thermal Response Test Calibration

The TRT simulation initially used material parameters from table 2 in the baseline case. The baseline thermal response was too high to be considered a match with the experimental values. It is believed that the differences in the responses between the baseline case and the experimental case are due to inaccurate TC laboratory measurements. The laboratory thermal conductivity test results (Table 1) of the thermal grout and the pile

structural grout have the same TC values, this could be the result of an inaccurate TC test. The TC of the pile is what affects the initial temperature response during the first segment of the TRT because the pile is the first domain to encounter a heat flux from the loops. The slopes of the temperature response after the initial temperature increase are approximately the same.

The TC measurement done on the field test samples might have produced a TC measurement that was lower than the actual value. The TC testing procedure used at the test site was the thermal needle probe procedure[38]. The thermal needle probe procedure uses a needle that is inserted into the material being measured and simulates a linear heat source. The probe applies a known current and voltage to the specimen and is equipped with a temperature measurement device to measure the temperature response. The temperature response is used to calculate the thermal conductivity of the material. This method could have significant error when measuring hard materials such as hard rocks or the grout used in the pile. When used to test hard specimens a hole must be predrilled to insert the probe and make the measurement. This leaves room for error with the contact surface between the probe and the sample. If the probe is inserted into a hole without good contact with the specimen than the resulting gaps between the concrete and the probe will result in a lower TC value.

The TC value of the pile was increased parametrically by 10% from the baseline case (Table 3) until the CFD results captured the experimental data. Increasing the pile TC had the desired effect of bringing the CFD results closer to the experimental values.

Table 3: parametric variations in the thermal conductivity of the 30cm pile

30cm Pile	*Thermal Conductivity [W/m K]*
Baseline	1.35
+10% TC	1.485
+20% TC	1.62
+30% TC	1.755
+40% TC	1.89
+50% TC	2.025

In addition to the possible error as a result of the TC measurement, the input heat rate is being directly applied to the fluid before it enters the earth domain with the exact experimental heat rate values. The simulation uses the experimental heat rate calculated using Equation 13 from the experimental voltage and current data, which suggests that the heater is 100% efficient at transferring electrical energy into thermal energy in the fluid.

$$Power = Voltage * Current \tag{13}$$

The assumption is also made that there is no heat gain or loss from ambient effects when using the heat rate values found from the voltage and current data. In reality the heater is not 100% efficient and there will be ambient heat loss within the system. The ambient heat loss occurs inside the test unit and when the fluid flows above ground through the pipes that attach the TRT unit to the pile. Most test units measure the inlet and outlet flow of the circulation fluid as it enters and leaves the test setup, not as it enters and leaves the pile. The test unit pictured in Figure 9 used for the Berkel test site, samples the inlet and outlet flow temperature inside the test unit, making any ambient effects built into the measured experimental temperature response. An ideal TRT unit would sample the temperature of

the circulation fluid directly at the inlet and outlet of the pile and also directly at the fluid heater inlet and outlet.

To simulate the possible effects of the heater efficiency and ambient effects between the heater and the pile inlet and outlet on the temperature response a reduced heat rate input was simulated with a 50% increase in the TC of the pile. The experimental heat rate values were reduced to 95% of their original value. The reduction in the average input heat rate can be seen in Table 4.

Table 4: The average CFD input heat rate values for 100 and 95% efficiency

EFFICIENCY	AVERAGE CFD INPUT HEAT RATE [W]
100%	2219.05
95%	2108.10

The heat rates as a function of time in Figure 15 correspond to the values in Table 4. The heat rate fluctuations are small compared to the total value.

2.3 CFD Thermal Response Test Results

The CFD model was able to reproduce a temperature response similar to the experimental results by varying the TC of the pile and the efficiency of the input heat rate.

2.3.1 CFD versus Experimental Results Comparison

The exact TC values of the soil and pile are difficult to know without more extensive testing of local samples. Accurately replicating the stratified soil condition surrounding the GEP also provides challenges because of the lack of precision associated with the soil sample locations and soil layer boundaries. The heater efficiency was not recorded with the experimental data and the earth inlet and outlet temperatures were

measured at the testing unit, not at the physical entrance and exit to the GEP. This leaves uncertainty and cause to believe a certain degree of systematic error is associated with the heat rate input and the temperature response during the TRT.

The experimental input heat rate and the CFD input heat rate at 100% and 95 % are plotted as functions of time in Figure 15. The experimental heat rate was sampled over 1100 times during the course of the simulation, the CFD simulation solved 570 time steps to simulate the same time period. The CFD solver used an interpolator to closely follow the input heat rate trend with only half the number of time steps. It was important to make the time steps small enough so that all of the input heat rate fluctuations would be captured in the simulation, Figure 15 illustrates how well the CFD simulation was able to reproduce the experimental heat rate.

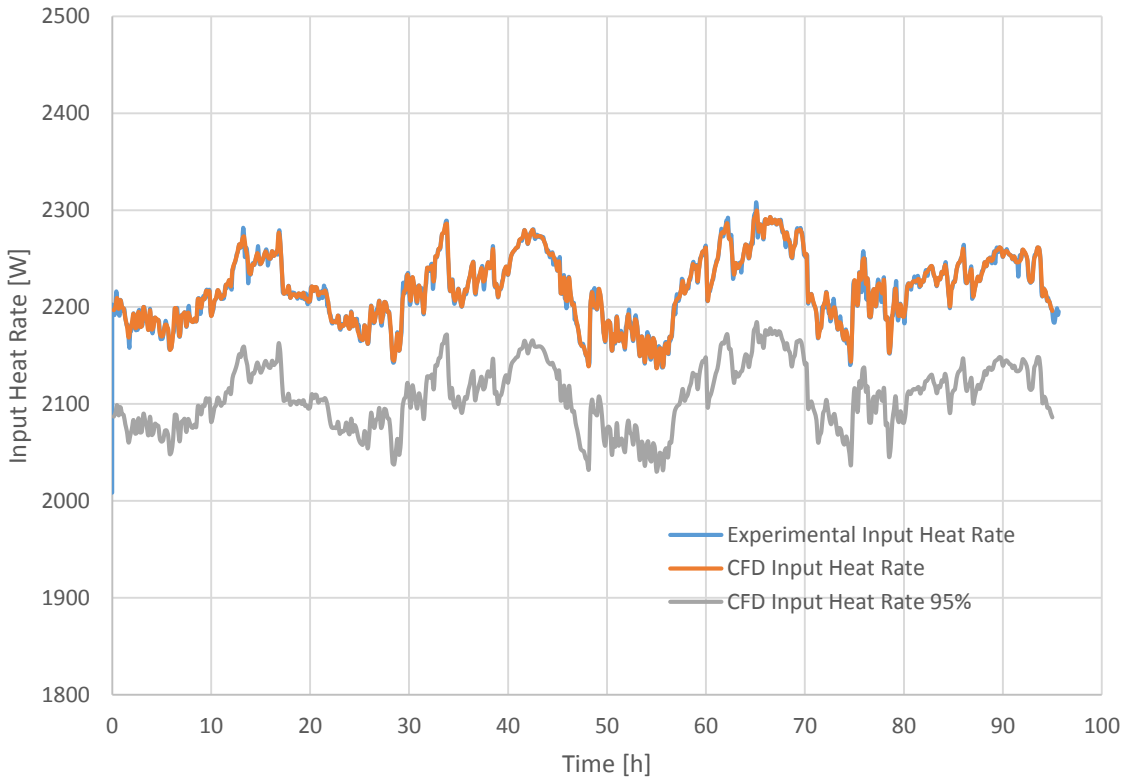

Figure 15: The experimental input heat rate and the CFD solvers interpolated input heat rate.

The experimental heat rate peak fluctuation is within ±5% from the average value. This is within the maximum allowable fluctuation of ±10% based on the recommendations set by Kavanaugh [26] for borehole TRTs. The magnitude of the heat rate fluctuations can be seen in Figure 15.

The average of the earth inlet and outlet temperatures for each of the tested cases and the experimental case are plotted in Figure 16 with the input heat rate. As the TC increased from the baseline case, its effect on the temperature response became less. The parametric variation of the pile TC brought the simulated thermal response within one degree Celsius of the experimental thermal response. A 5% inefficiency was then added to the input heat rate to simulate the inefficiencies in the fluid heater and the insulation of the pipes. The results of the 50TC with 95% efficiency case are slightly lower than the experimental values. It is believed that the TC values of the pile and of the soil as well as the efficiency of the system could be tweaked to produce an exact match with the experimental values. It is impossible to know the exact TC values of the earth surrounding the soil and the efficiency of the test setup as recorded. Knowing this, any experimental GEP test results would be difficult to reproduce exactly with a numerical model. However the CFD results were similar to the experimental results after making good engineering assumptions about the test.

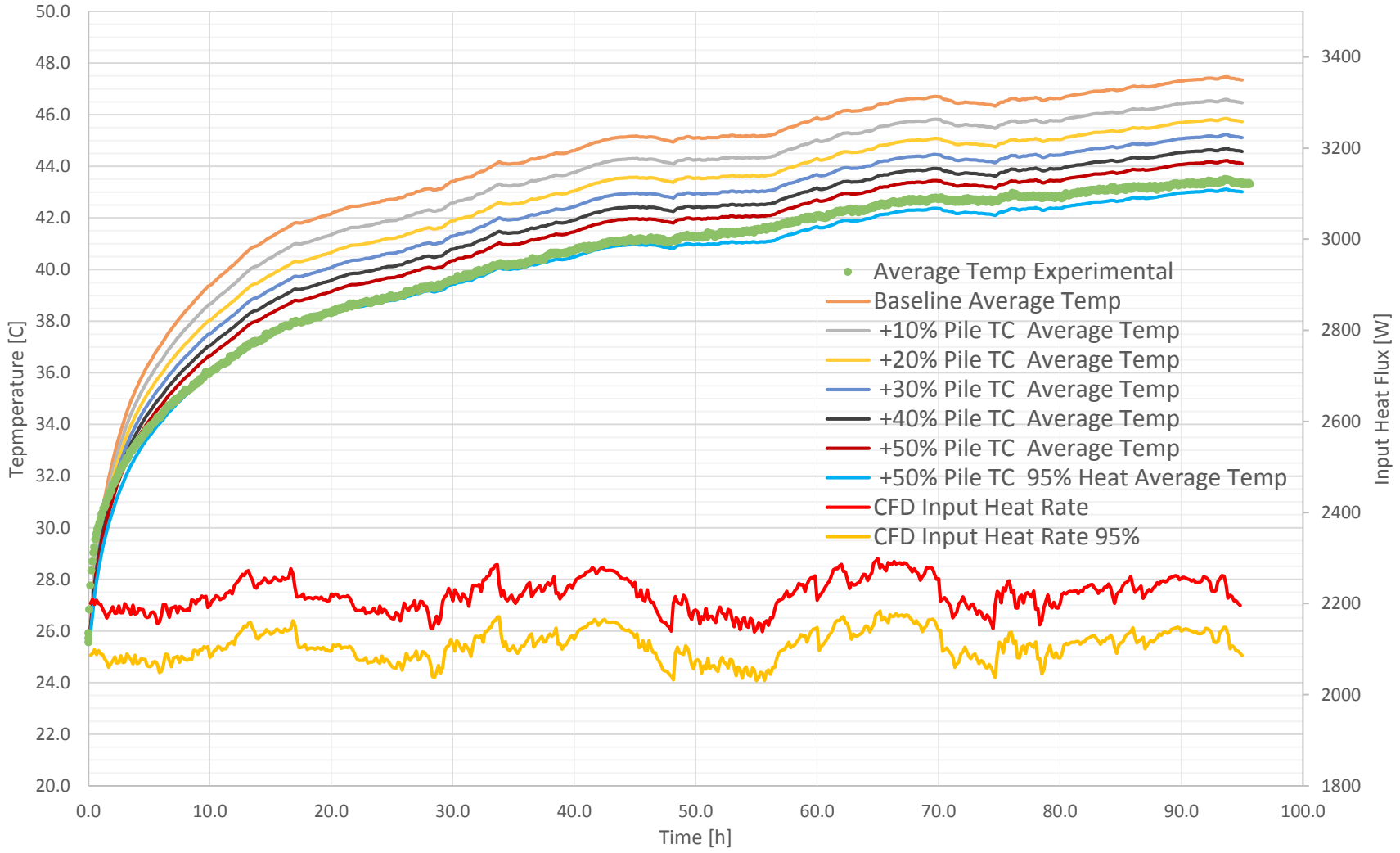

Figure 16: The average temperature results of the 30cm pile CFD simulations with parametrically variations and experimental results.

The total calorimetric power of the GEP was measured as a function of the total heat flux leaving the fluid. The input heat rate to the fluid and the total heat flux out of the fluid into are plotted in Figure 17. The fluid wall heat flux takes approximately 10 hours to match the level of the input heat rate. The heat rate from the fluid is 10W less than the input heat rate on average or one half of a percent less. It is expected that the heat rate leaving the fluid will be slightly less than the input heat rate.

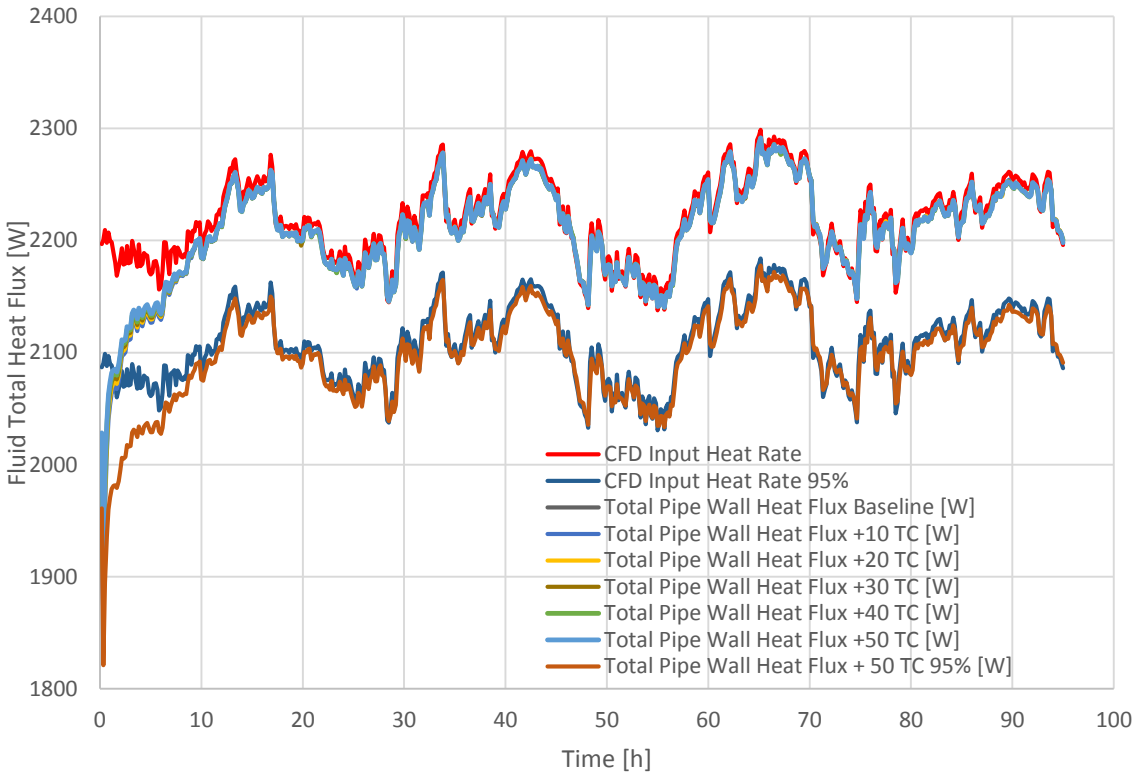

Figure 17: The total heat flux or heat rate leaving the fluid of the 30cm pile CFD simulation.

The total heat flux through the pile wall as a function of time was also measured and can be seen in Figure 18. The heat flux through the pile wall takes much longer to develop than the heat flux out of the fluid. The heat flux at the pile surface does not approach the input heat rate until after 30 hours. The heat transfer through the pile surface is expected

to have a delayed reaction from the input heat rate because of the time required for the interior of the pile to absorb heat from the fluid.

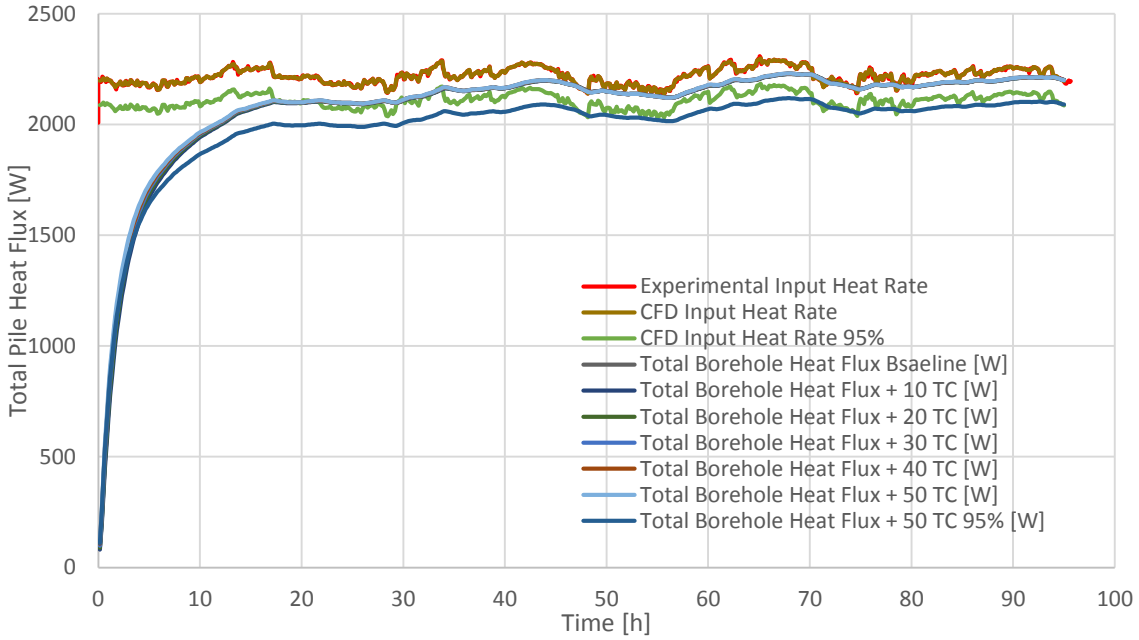

Figure 18: The total heat flux or heat rate leaving the pile surface of the 30cm pile CFD simulation.

The thermal resistance of each of the cases was measured and plotted as a function of time and can be seen in Figure 19. The pile thermal resistance calculated using Equation 10 reaches its steady state value close to 20 hours. It can be seen that the pile thermal resistance has a noticeable variation when the thermal conductivity of the pile is changed. As the thermal conductivity of the pile increases the borehole thermal resistance decreases. The pile thermal resistance reaches steady state close to the same time the total heat flux through the borehole approaches the input heat rate. The pile thermal resistance remains constant after the temperature differential between the fluid and pile surface temperature becomes constant.

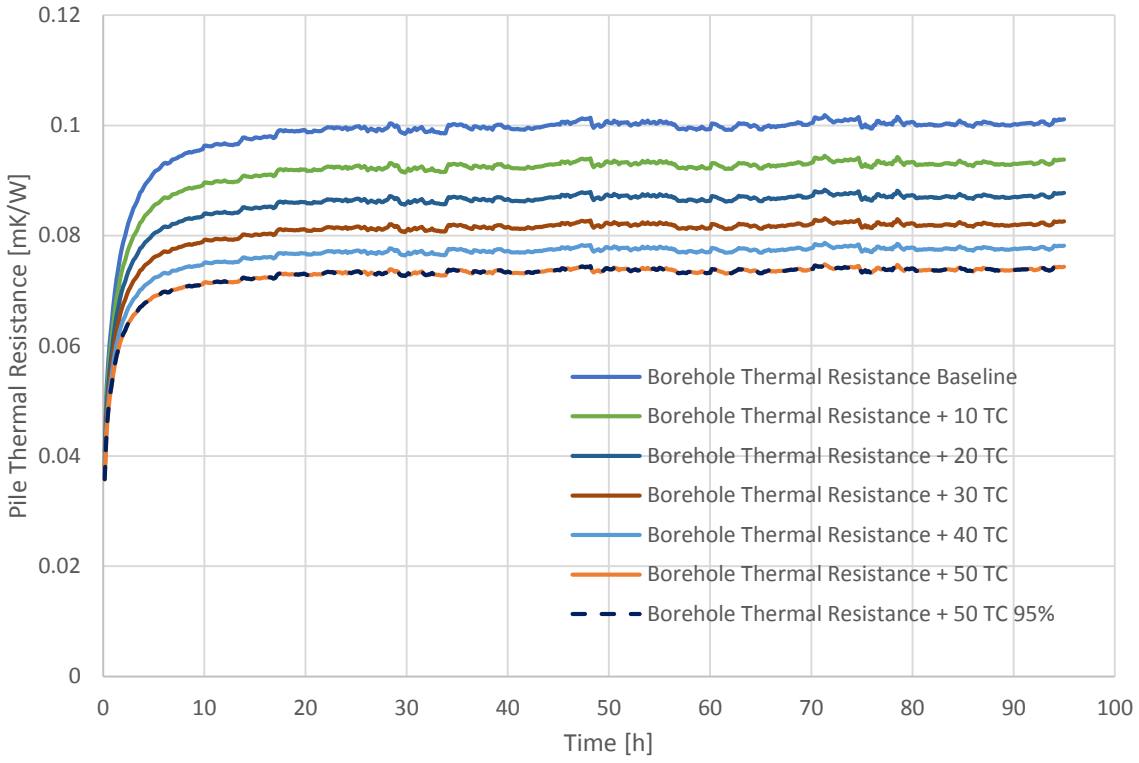

Figure 19: The pile thermal resistance of the 30cm pile CFD simulations.

To measure the error between the temperature response of the CFD simulation and the experimental results the average temperature of the last hour, last five hours, and last ten hours of the simulation were compared to the experimental results. The error of the last hour, the last five hours and the last ten hours are similar for each of the simulations. The error steadily decreases from 9.2% in the baseline CFD case to less than 1% in the +50TC with 95% heat rate efficiency case (Figure 20).

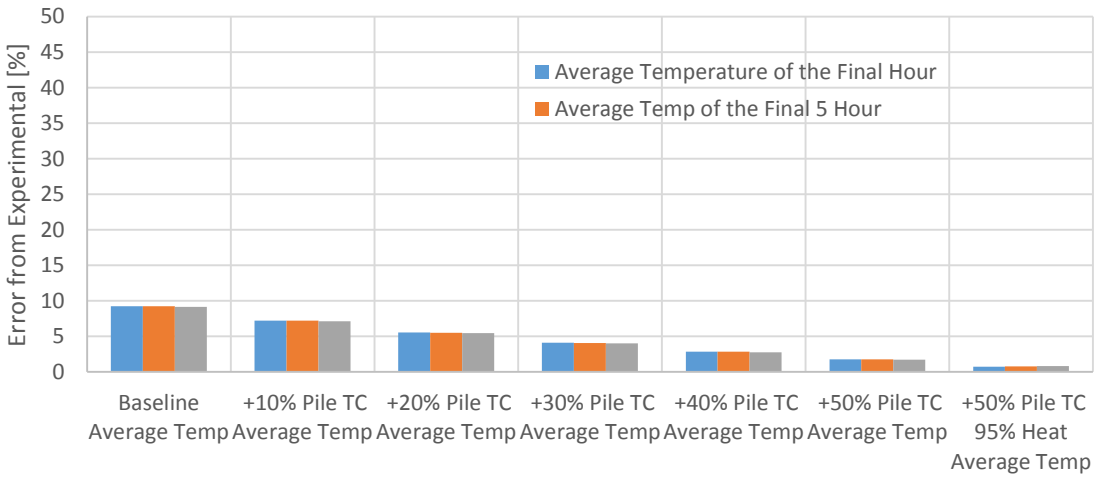

Figure 20: Final temperature error between the CFD simulations and the experimental results

The error of the response was also measured by the slope of the temperature response after some initial amount of time. After some initial time defined by the geometry of the pile the temperature response of the fluid will become linear on a semi log scale. The experimental results and the CFD results are not exactly linear as a result of the input heat rate fluctuations. In reality the input heat rate cannot be constant but the trend lines in Figure 21 illustrate how the temperature response shows a linear trend on a semi log plot.

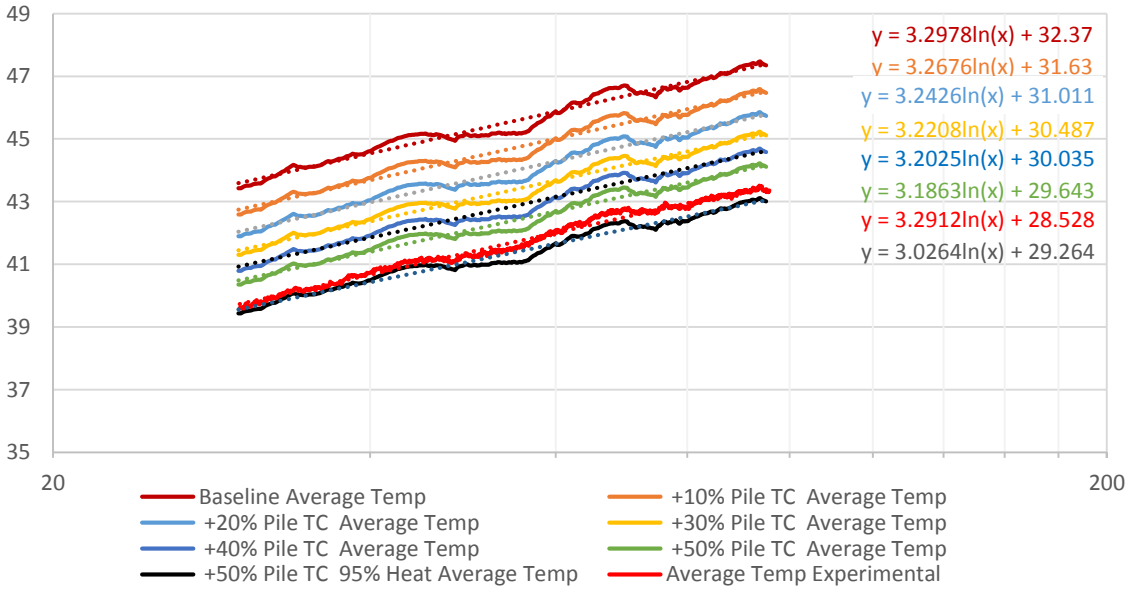

Figure 21: Error of the 30cm pile final temperature response slope

The slope of the baseline case most closely matches the experimental case's thermal response (Table 5). The relationship between the TC of the soil and the concrete is most similar to the experimental case in the baseline case. However the final temperature value of the baseline case is the farthest from the experimental value.

Table 5: Error of the 30cm pile final temperature response slope

Test Case	*Slope of Thermal Response after 30 hours*
Baseline	3.2978
+10 TC	3.2676
+20 TC	3.2426
+30 TC	3.2208
+40 TC	3.2025
+50 TC	3.1863
+50 TC 95%	3.0264
Experimental	3.2912

One possibility for this could be that the TC measurements of all the samples could have been measured lower than the actual values systematically. In addition the efficiency of the input heat rate was not tested at TC values lower than plus 50TC and only a 95% efficiency case was tested. In reality the efficiency could be less than 100% but higher or lower than 95%. It is reasonable that a combination of more accurate slope and final temperature values could be achieved with slight tweaks to the pile TC value and the heat rate efficiency

2.3.2 Fluid Flow Field Analysis

The CFD model was able to capture the experimental data with its results by parametrically varying the pile TC and the heat rate efficiency. Additionally the CFD simulation solved the fluid flow through the GEP. The heat transfer and the flow characteristics of the fluid are solved simultaneously with the earth domain's thermal response. Discretizing the fluid domain and solving the flow characteristics provides

additional insight into how the GEP systems function. Some basic flow parameters of the 30cm pile are shown in Table 6.

Table 6: Flow characteristics of the 30cm GEP CFD model

	Flow Rate [l/min]	Velocity [m/s]	Reynolds number
30cm Energy Pile	33.7	0.96	26000

Figure 22 show streamlines through the fluid domain. The streamline color is representative of the temperature of the fluid at that point along the stream line. The streamlines are shown from the final time step of the simulation. The streamlines clearly show mixing taking place directly after the fluid leaves the heated length and flows into the earth domain. A close up of the flow leaving the heated length and entering the earth domain is shown enlarged where mixing can be seen.

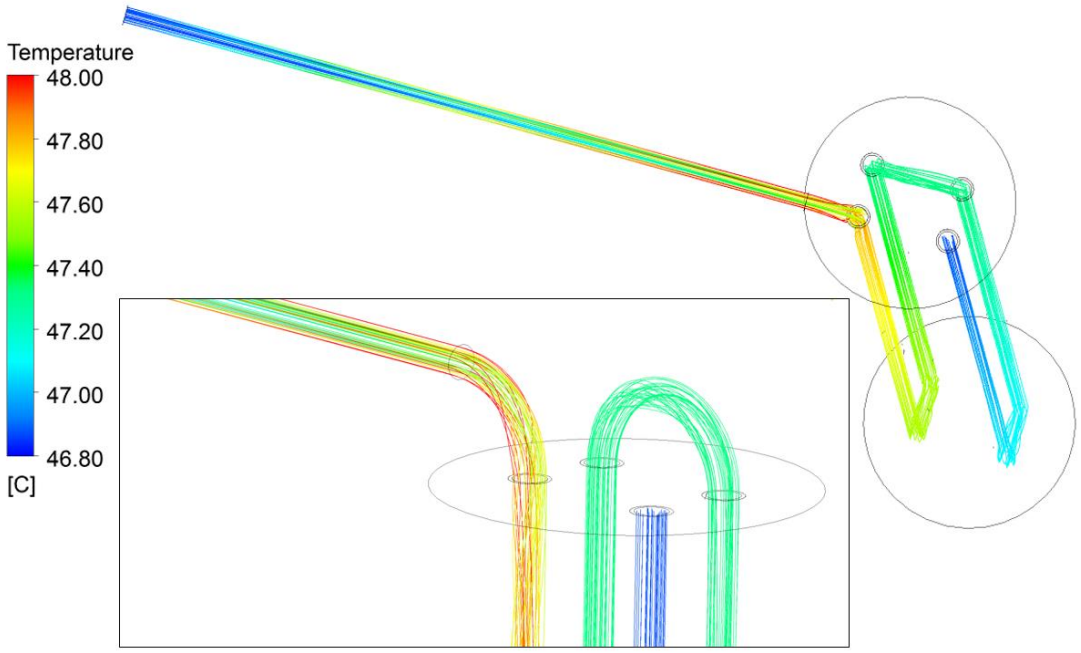

Figure 22: Flow streamlines with in the fluid domain with an enlarged image of the top of the pile.

The temperature of the streamlines is plotted versus pile depth in Figure 23. The mixing can be seen taking place at the top of the plot where the fluid enters the first HDPE pipe.

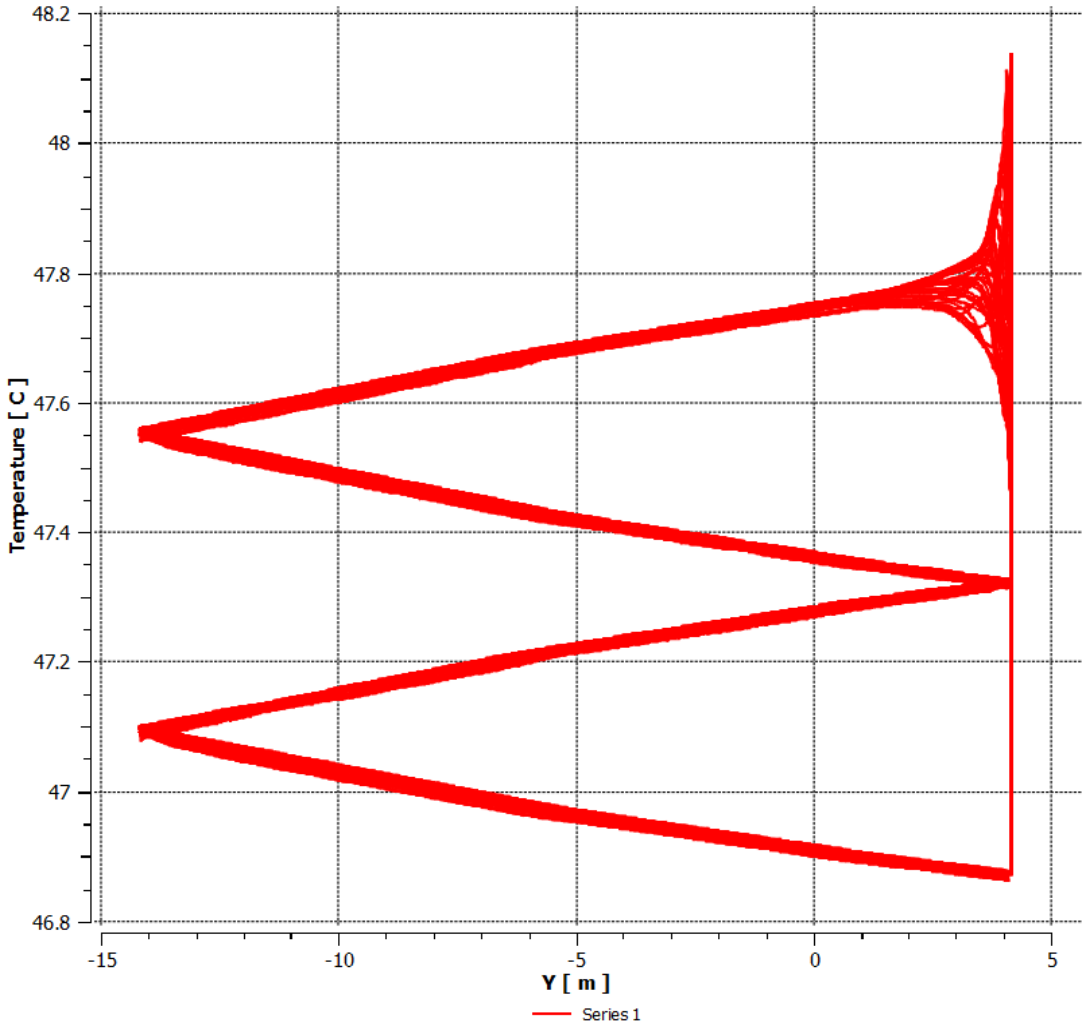

Figure 23: The temperature of fluid streamlines plotted versus pile depth.

The temperature distribution along the lengths of HDPE pipes shows a linear temperature trend through the pipe circuit. The velocity of the flow in the 30cm double loop experimental test and the CFD simulation was 0.96m/s. The linear temperature distribution through the pipe circuit is verified by Markiewicz who showed that using a high flow rate, close to 1 m/s, will produce a linear temperature distribution through the circulation pipes. [10, 42]

In Figure 24 the velocity profile shows the velocity in the vertical direction at a depth of 10m in one of the HDPE pipes. A fully developed velocity profile is seen with the greatest velocities in the center as expected and smaller velocities approaching a wall velocity of zero around the edges due to the no slip wall conditions.

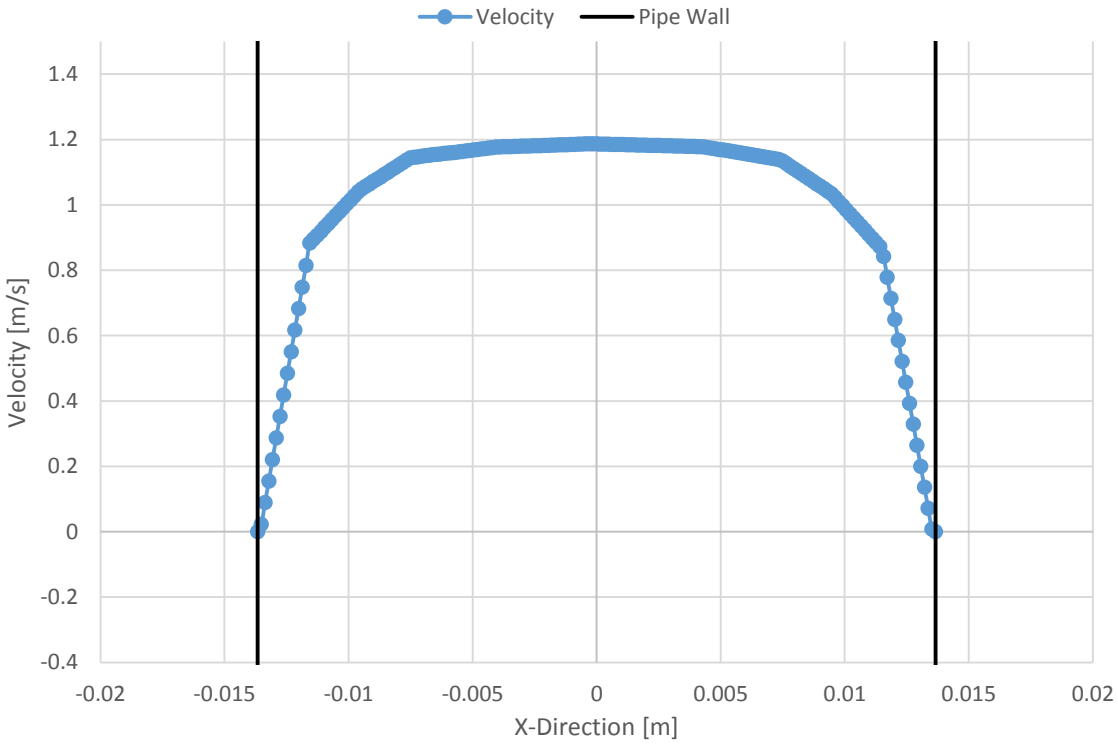

Figure 24: velocity profile shown at the mid-plane of one HDPE pipe.

The pressure drop through the HDPE pipe is a key component in the performance of the energy pile that CFD analysis solves. The 30cm GEP produced a total pressure loss of 26.8 kPa in the CFD simulation. Figure 25 shows how the pressure drops through the pile with a plot of the pressure drop vs. depth of the pile with zero being ground level.

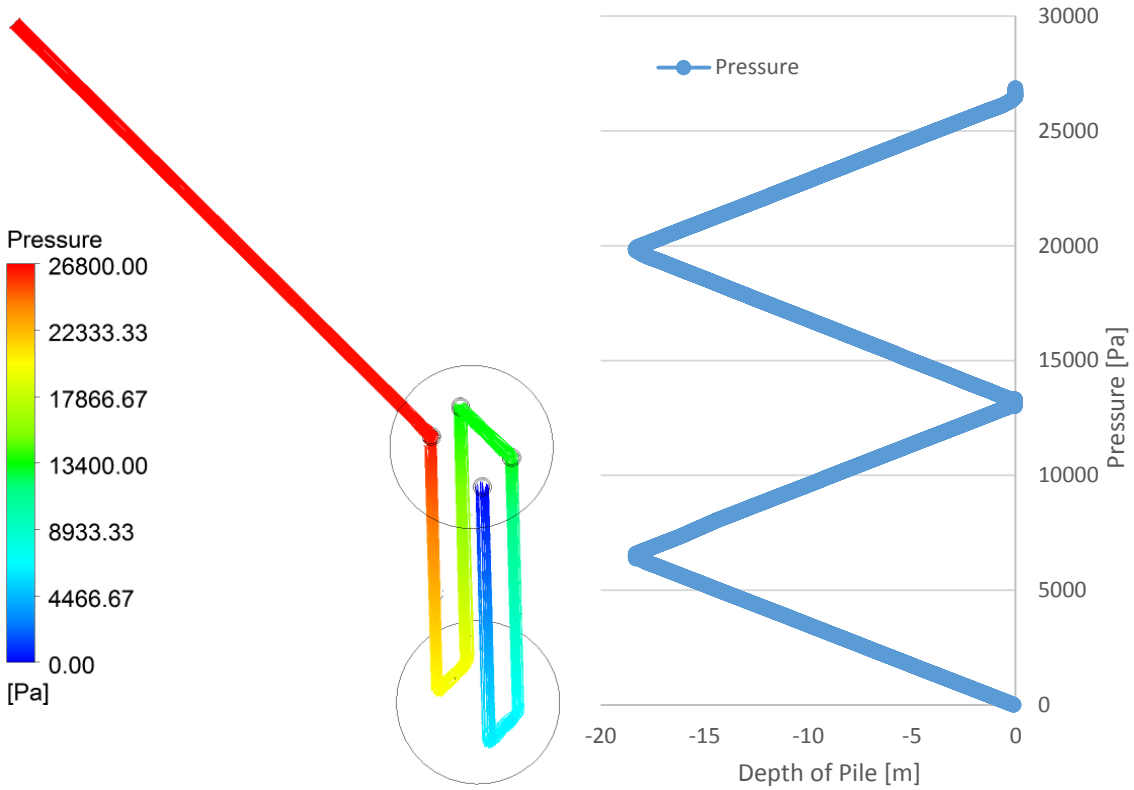

Figure 25: The pressure drop through the GEP pipes.

The necessary pumping power needed to overcome the pressure drop through the loops is a key factor in the efficiency of the system. Larger pressure drops will require larger pumps with more pumping power that use more energy.

Chapter 3: Large Diameter Energy Pile Analysis

Large diameter piles differ from boreholes because of their length to diameter ratio. BHE systems have a high length to diameter aspect ratio while large diameter GEP systems have much lower length to diameter aspect ratios. GEP systems are in their early stages of research compared to the amount of research done on BHEs. GEP systems although they are being more widely implemented still do not have robust standards or guidelines in place to aid in the design of the systems. The analysis in this section aims to provide better understanding of large diameter pile performance

3.1 Large Diameter Energy Pile Background

The large diameter energy piles analyzed in this chapter are 60cm, 120cm, and 180cm in diameter. The geometry is based off of recommendations made by the U.S. Department of Transportation Federal Highway Administration for drilled shafts in the Drilled Shafts: Construction Procedures and LRFD Design Methods Manual [43]. Energy pile geometry is more complicated than conventional borehole design because energy piles contain structural steel reinforcement. The steel reinforcement rebar must be designed based on the loads and stresses imposed by the structure it is supporting. This study uses a general case with the dimensions for the energy piles based on preliminary design recommendations.

3.2 Large Diameter Analysis Cases

Five cases were studied with the large diameter energy piles that break down into two separate groups. The simulation length for each case is ten days or 240 hours. The five cases are listed below in Table 7. In each case the pipe center to pile surface spacing

is defined based on the preliminary design of the rebar reinforcement in the pile. For preliminary design purposes the concrete cover is chosen based on the minimum cover recommended by the FHWA for a given pile diameter. The concrete cover of a pile is the thickness of the concrete outside of the steel reinforcement cage. The FHWA recommends that that the cover for drilled shafts be a minimum of 3inches (7.62cm) for shafts up to 3ft (91.4cm), 4inches (10.16cm) for shafts from 3 to 5ft (91.4 to 152.4cm), and 6inches (15.24cm) for shafts greater than 5ft (152.4cm). The minimum cover and the required spacing for the necessary rebar reinforcement cage defines the spacing between the pile surface and the HDPE pipes. The pipes are installed on the inside of the rebar reinforcement cage as shown in Figure 6.

Table 7: General geometry specifications for each of the large diameter piles.

Large Diameter Energy Pile Cases				
Case	Diameter [cm]	Number of Loops	Pile Center to Pipe Center [cm]	Pipe Center to Pile Surface [cm]
1	60	2	17.5	12.5
2	120	4	44	16
3	120	5	44	16
4	120	6	44	16
5	180	6	68	22

3.2.1 Geometry and Mesh for large diameter piles

The large diameter pile cases all have identical parameters except for the diameter of the piles and the number of loops. There are two different comparison sets for the large diameter cases, varying diameter and varying number of loops. The varying diameter case includes cases 1, 2 and 5 from Table 7 listed above. These cases were 60cm, 120cm and

180cm in diameter respectively. The second comparison was between constant diameter piles and includes cases 2, 3, and 4. The number of loops was varied in these three simulations each with a diameter of 120cm but with 4, 5, or 6 loops inside the pile. The rest of the parameters are constant between all of the large diameter pile simulations. The material properties for the materials used in the large diameter pile cases can be seen in Table 8.

Table 8: Material properties of the large diameter simulations solid domains.

Material	*Thermal Conductivity [W/m·K]*	*Specific heat [J/kg·K]*	*Density [kg/m^3*
HDPE	0.39	2300	960
Concrete	1.50	1200	2500
Soil	2.00	1500	2000

The dimensions of the soil domain and of the HDPE pipes can be seen in Table 9 as well as some additional information that is consistent between all of the large diameter cases. The mesh in the large diameter models was focused on creating the smallest number of cells possible while maintaining a convergence criteria of $1.0x10^{-5}$. The meshing principles and strategies used for the large diameter cases are the same as those discussed in Chapter 2. The mesh was an unstructured mesh that used inflation layers in the fluid boundary layer region and hex-dominant meshing method in the pile and the soil domain. The hex-dominant method was used to decrease the number of cells in the larger domains. The inflation layers inside the fluid domain helped the convergence of the boundary layer and heat transfer with in the fluid domain.

Table 9: Constant dimensions and parameters of the large diameter analysis

HDPE Pipe Dimensions		
Inside diameter	3.4	cm
Wall thickness	3.8	mm
Outside diameter	4.2	cm
Roughness	0.0015	mm
Earth Dimensions		
Soil Diameter	25	m
Soil Depth	30	m
Other Information		
Heat rate	100	W/m
Fluid flow rate	10	l/min
Pile length	20	m
Total heating power	2000	W
Simulation time	240	h

3.2.2 Boundary Conditions

The large diameter CFD models were set up with initial conditions and boundary conditions similar to the model described in Chapter 2 but with different values. The initial temperature condition of all domains in the large diameter models was 12℃. The surfaces of all the solid domains at or above ground level had an adiabatic boundary condition imposed on them. The adiabatic condition was imposed on the ground level surface of the soil domain, the piles, the exposed ends of the HDPE pipes, and loop connectors that are above ground. The adiabatic ground level condition was imposed because this model is not simulating the effects of the ambient air temperature or solar heat gain. The boundary

condition of the outer walls was a fixed temperature condition of 12℃ for the entire 240 hour duration of the transient simulation. The fixed temperature boundary condition simulates the earth as an infinite heat sink. The fluid inlet temperature was set equal to the fluid outlet temperature to simulate a recirculating flow. The constant input heat rate was applied to the heated length of fluid just after the fluid inlet.

The fluid flow conditions were set up to model the heat transfer and thermal behavior of the flow as accurately as possible. The inlet flow field was set to a constant 10 l/min and the outlet flow pressure was constrained to a static pressure of zero Pa. The pressure constraint on the outlet flow shows the total pressure loss through the system with the highest pressure at the model inlet. The flow was modeled with a no-slip wall condition at the pipe walls and a wall roughness of 0.0015mm. The no-slip wall condition holds the near wall velocity to zero.

3.3 Large Diameter Piles with Varying Diameters

The large diameter pile cases with varying diameters each produced unique thermal responses. The larger the diameter of the pile the longer it takes for the piles heat transfer rate to reach a steady state. There were three different diameters tested in this comparison, 60cm, 120cm, and 180cm. The 60cm GEP was the smallest diameter and had the smallest number of loops as well. As the diameter gets larger the number of loops increased to maintain an equal loop density for the comparison. The 60cm case has two loops, the 120cm case has four loops and the 180cm case has six loops. Figure 26 shows the geometry of all three cases, the earth domain and the 60cm pile can be seen in the left side of the image. The right side of the image shows enlarged sections of the top of the piles and the bottom of the piles so that the HDPE pipe loop configurations for each case can be

visualized. The HDPE pipes are equally spaced around the pile in each case. Figure 27 shows the layout of each pile from a top view with the diameters and distances between the center of the pipes and the center of the piles labeled. The distance between the HDPE pipes and the pile surface varies slightly between cases to account for constructability concerns as outlined by the FHWA[43]. The required concrete cover increases with the diameter of a structural pile. A concrete pile with steel reinforcement cage must have a sufficient concrete cover to protect the steel reinforcement from water intrusion and corrosion.

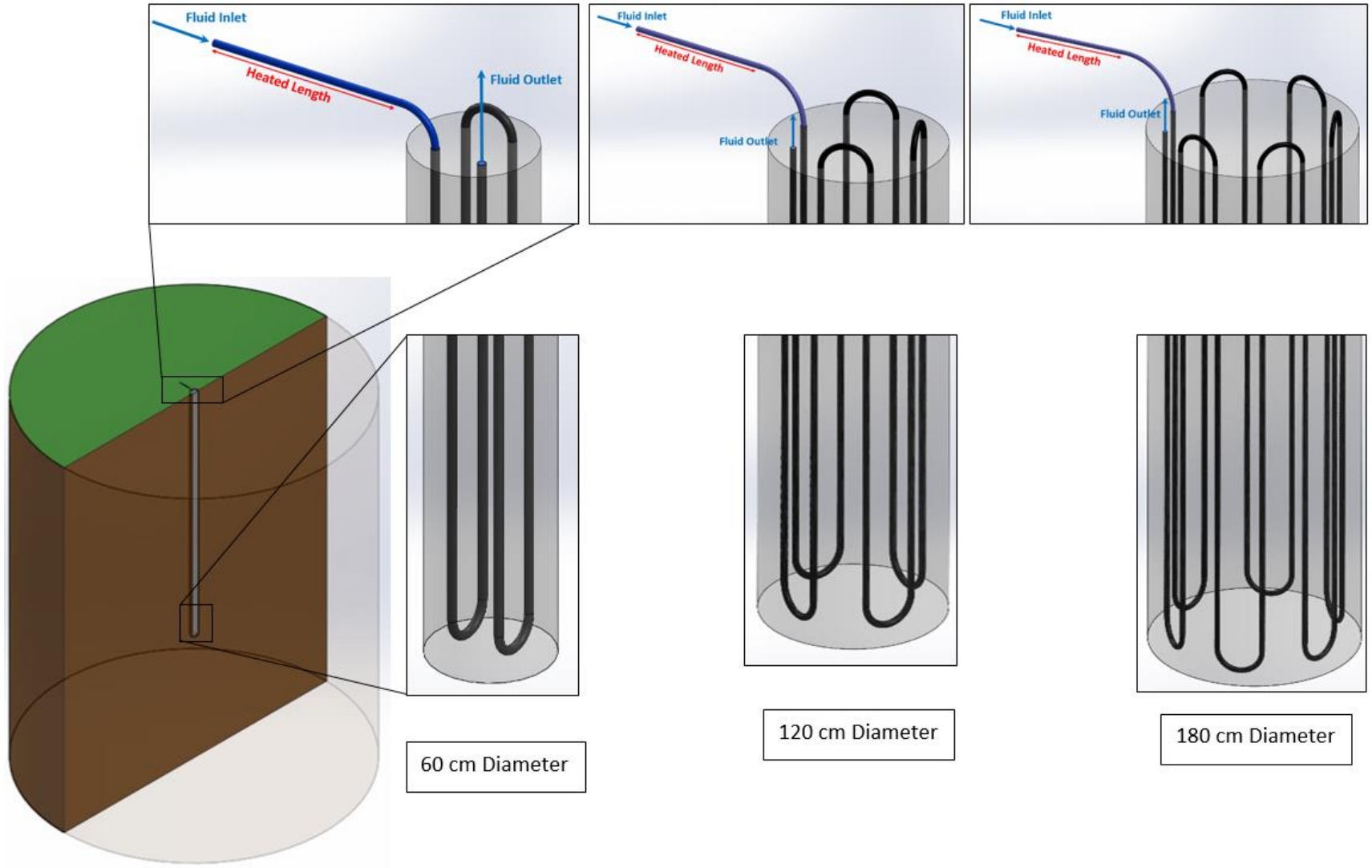

Figure 26: The geometry of the 60cm, 120cm, and 180cm piles with enlarged sections of the top and bottom of the piles.

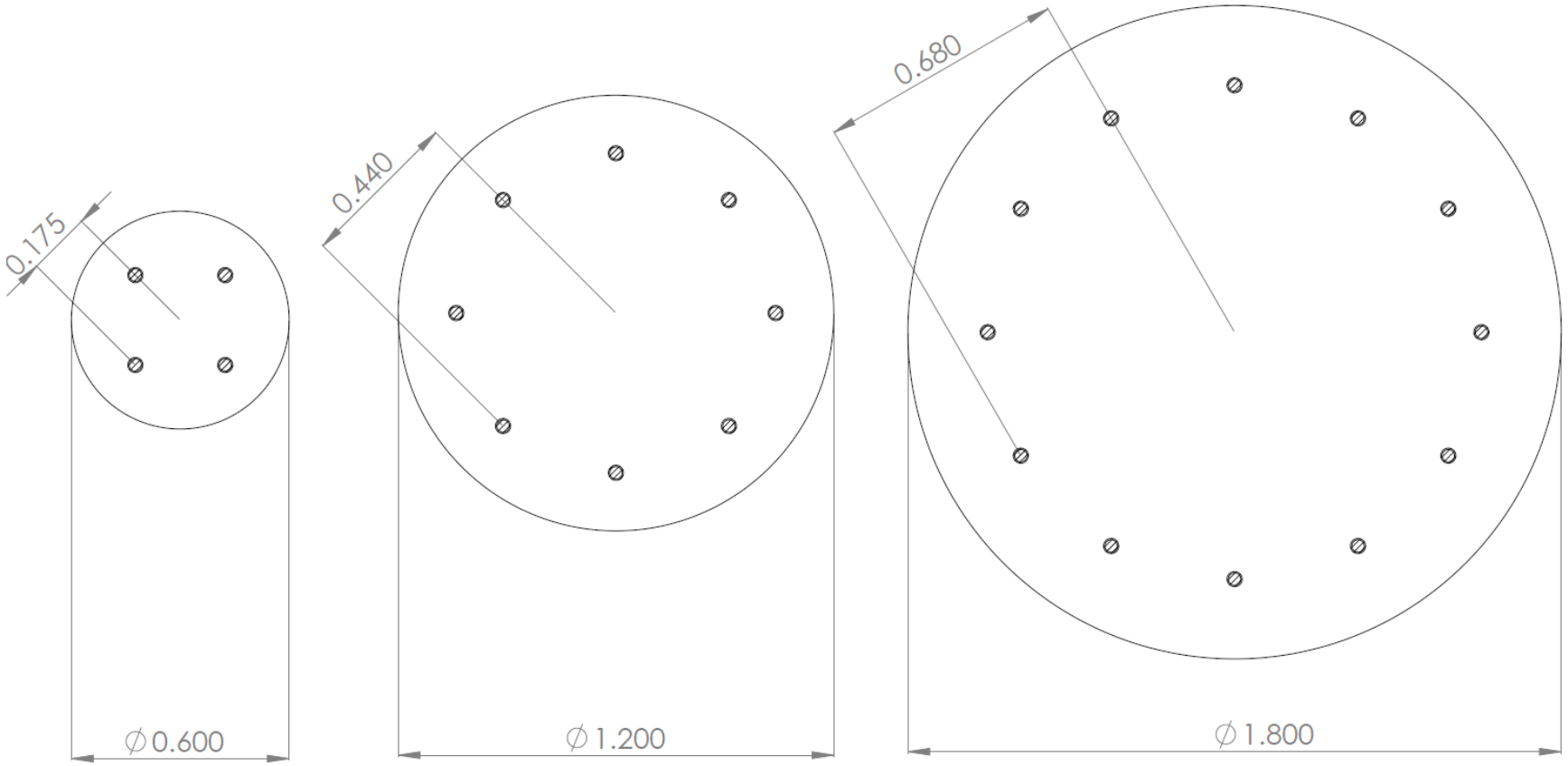

Figure 27: Top view of the 60cm, 120cm with 4 loops, and the 180cm pile showing the equal spacing of the HDPE pipes.

The temperature response as a function of time for the three cases in the varying diameter comparison are shown in Figure 28. The temperature response is tracked by measuring the average fluid temperature of the pile. The 60cm pile produced the highest temperature response. The 120cm case and the 180cm case produced much smaller average fluid temperature values over the course of the simulation. The fluid was injected with the same input heat rate but has a longer path to travel through the earth to dissipate heat when the diameter is larger and the pile has more loops. The greater the spacing between the HDPE pipes the less interference between the pipes. The length of the HDPE pipe and the spacing of the HDPE pipe contributed significantly to the thermal response of the fluid. The 180cm pile was a significantly larger thermal mass than the two smaller piles. This allowed the 180cm pile to absorb more heat and more effectively dissipate it to the surrounding soil. As the volume of the pile got larger the pile absorbed more of the input heat and resulted in a lower the temperature response.

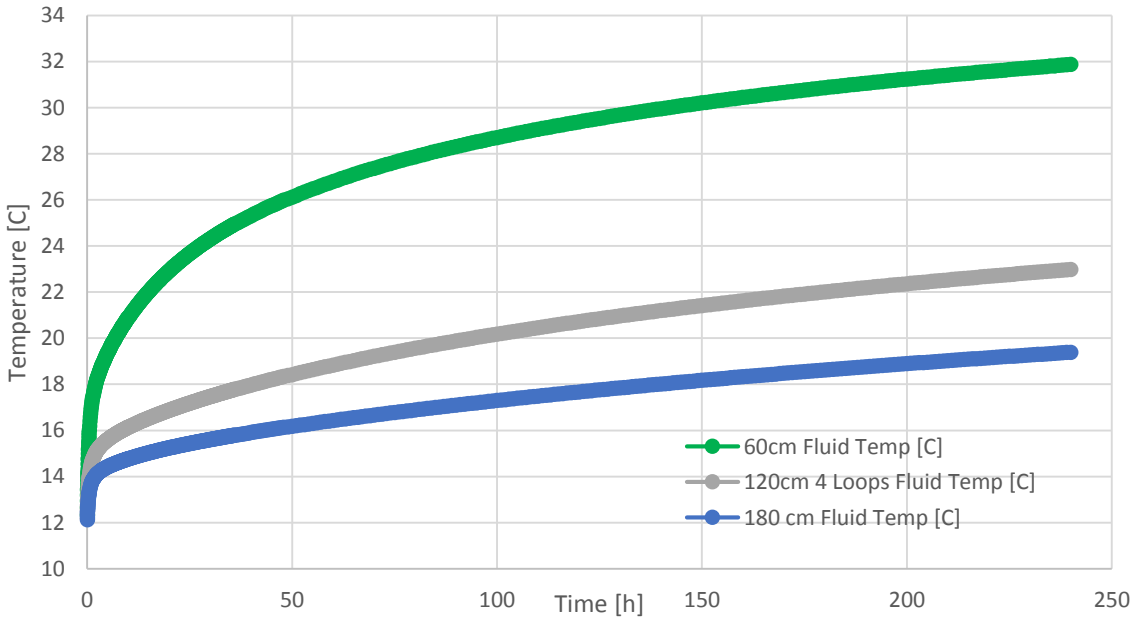

Figure 28: The Average fluid temperatures of the 60cm, 120cm with 4 Loops, and 180 cm case.

The temperature response was also looked at on a semi-log scale to show when the pile approaches a steady state heat transfer rate. Figure 29 shows the same information as Figure 31 but on a semi-log scale. The temperature curves will develop a linear trend when a heat transfer rate between the fluid and the pile surface has reached a steady state. The 60cm pile approaches a steady state after approximately one day. The 120cm case and 180 cm case did not reach a steady state heat transfer rate at the end of the analysis period of ten days. The fact that the 120cm and 180cm piles have not reached a log-linear trend after ten days suggests that the full thermal capacity of the piles have not been reached after ten days.

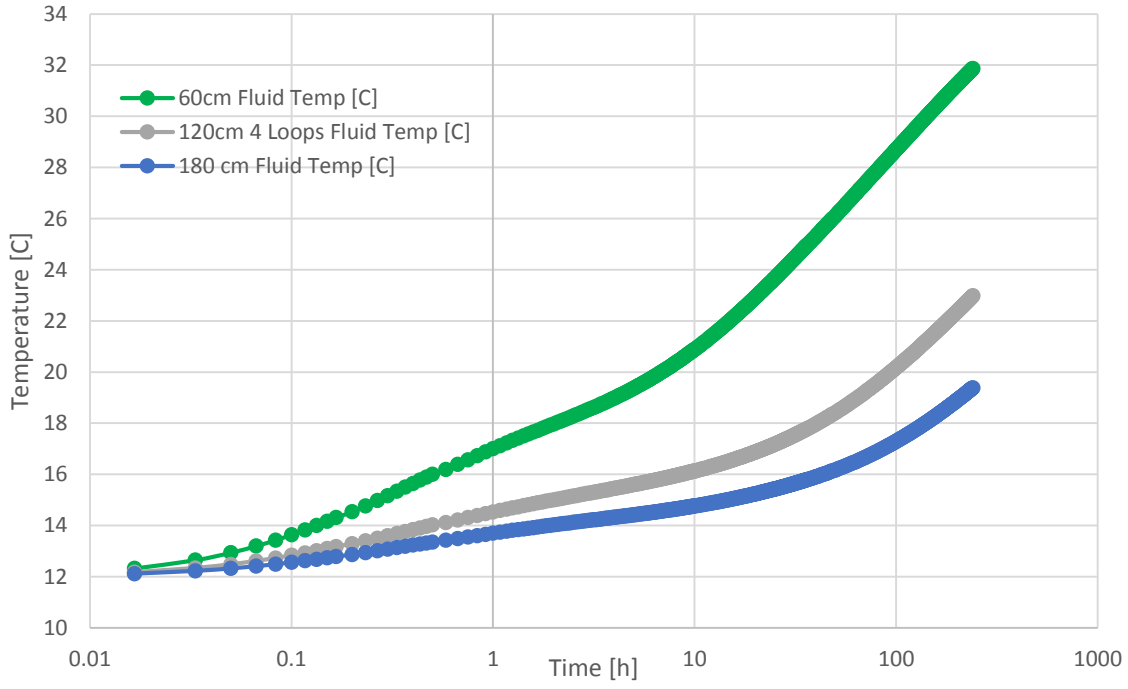

Figure 29: Average fluid temperature of the 60cm, 120cm with 4 Loops, and 180 cm piles on a semi log scale.

The fluid heat flux was calculated as the wall heat flux through the interface of the fluid and the HDPE pipe wall. The fluid heat flux was very similar for each of the three cases. For the first few hours the total fluid heat flux increased greatly and approached the input heat rate. As the diameter of the pile is increased the number of loops increases,

increasing the amount of pipe the fluid uses to dissipate heat to the pile. The length of HDPE pipe does not have a large effect on the total fluid heat flux. The fluid heat flux difference between these three cases is insignificant (Figure 30). The temperature differential between the fluid and the HDPE pipe used to calculate the fluid heat flux is insignificantly different between cases resulting in similar fluid heat flux values.

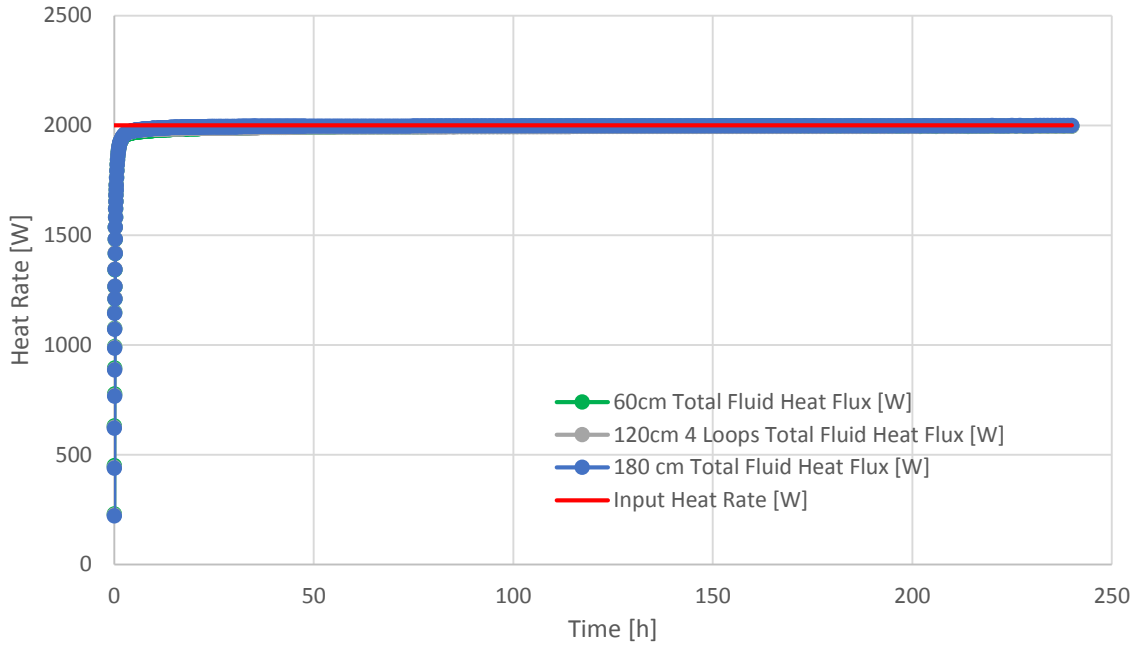

Figure 30: Fluid heat flux for the 60cm, 120cm with 4 loops, and 180cm cases.

The total heat flux through the pile surface of each case approaches a steady state value equal to the input heat rate after many days (Figure 31). The initial increase in heat flux through the pile surface was greater as the pile diameter got smaller. For the same 2000W input heat rate the heat transfer towards the edge of the pile surface in the radial direction happens fastest in the 60cm pile. The total pile surface heat flux approaches a steady state heat transfer rate faster as the diameter of the pile gets smaller. The heat flux through the pile surface is expected to become close to the value of the input heat rate after the full thermal capacity of the pile has been reached.

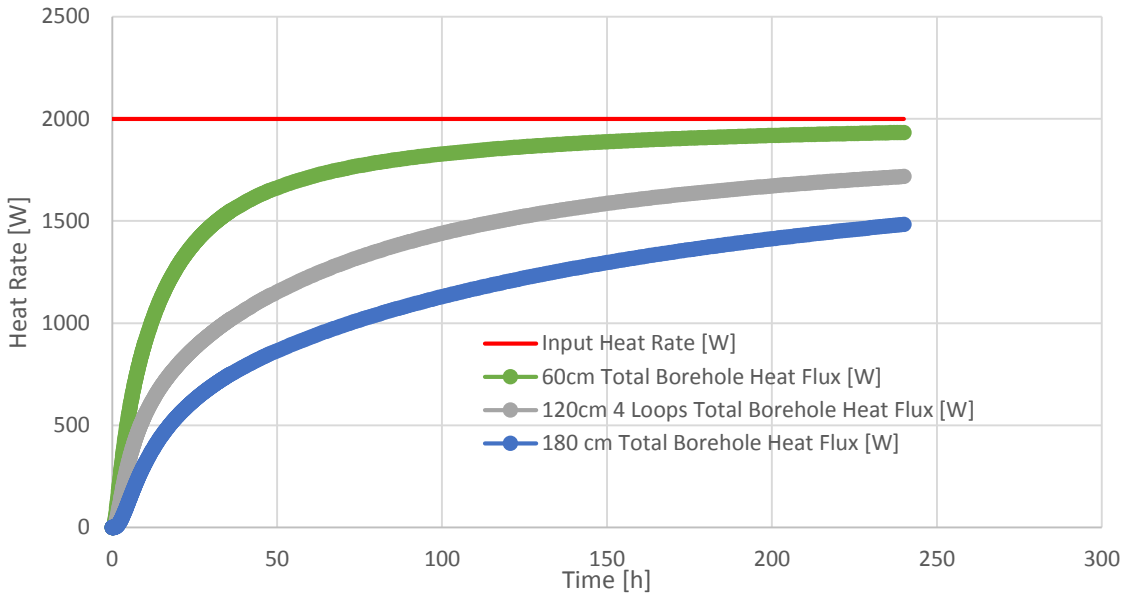

Figure 31: The total pipe heat flux for the 60cm, 120cm 4 loop, and 180cm cases.

The pile thermal resistance is an important parameter when designing new energy pile systems. Equation 10 was used to calculate the resistance which is a measure of the temperature difference between the pile surface and the fluid temperature. The pile thermal resistance for the three varying diameter cases can be seen in Figure 32. The resistance decreases as the diameter of the pile increases. In this comparison the variables in the resistance equation remain relatively constant between the three cases except for, the pile surface and fluid temperatures. The heat rate used was the simulated total fluid heat flux for all three cases as shown in Figure 30. The length of the pile is a constant 20m for all three cases. When calculating the resistance the difference between the pile surface temperature and the fluid temperature is the largest contributor to the resistance value. The 180cm pile is shown to perform the best under the conditions set in this comparison. The 180cm pile more effectively dissipates the injected heat rate than the 60cm pile and the 120cm pile with 4 loops.

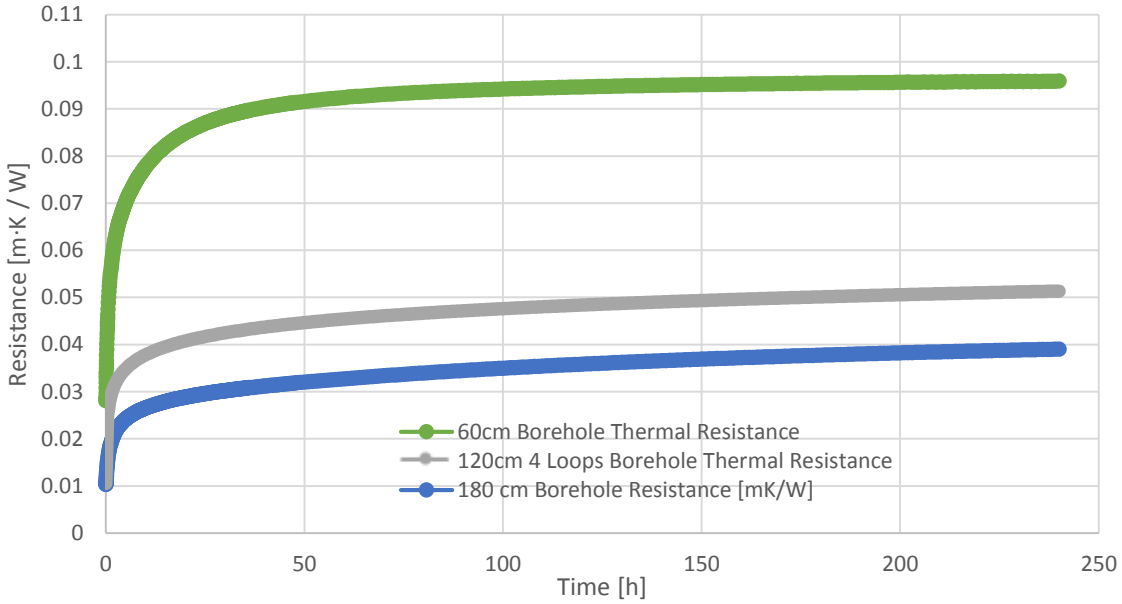

Figure 32: The pile thermal resistance values for the 60cm, 120cm with 4 loops, and the 180cm pile.

The finite line source method was compared to the temperature distributions in the outward radial direction from the pile surface. Figures 33-35 show the temperature distributions calculated with the CFD simulations compared to the values found using the line source method. The finite line source method and the 60cm pile simulation produce very similar results at each of the times measured 40h-240h, in 40h increments. The CFD simulation of the 120cm pile with 4 loops shows a much larger temperature response than the finite line source method early in the simulation. At later times, closer to 240h the finite line source method and the 120cm with 4 loops simulation show much more similar results. The CFD simulation of the 180cm pile shows a larger temperature response than the finite line source method at each of the compared times. In each case the CFD results and the results from the finite line source method are more similar after a longer duration of time. The finite line source data is only valid outside of the pile surface in the soil domain, for this reason the data starts at the edge of the pile surface and not at 0m.

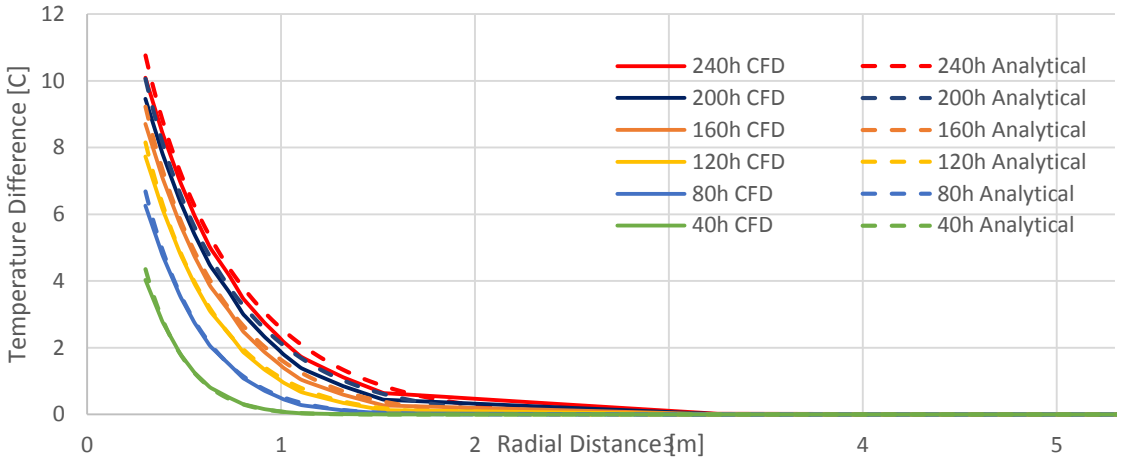

Figure 33: The 60cm CFD and finite line source method radial temperature distribution.

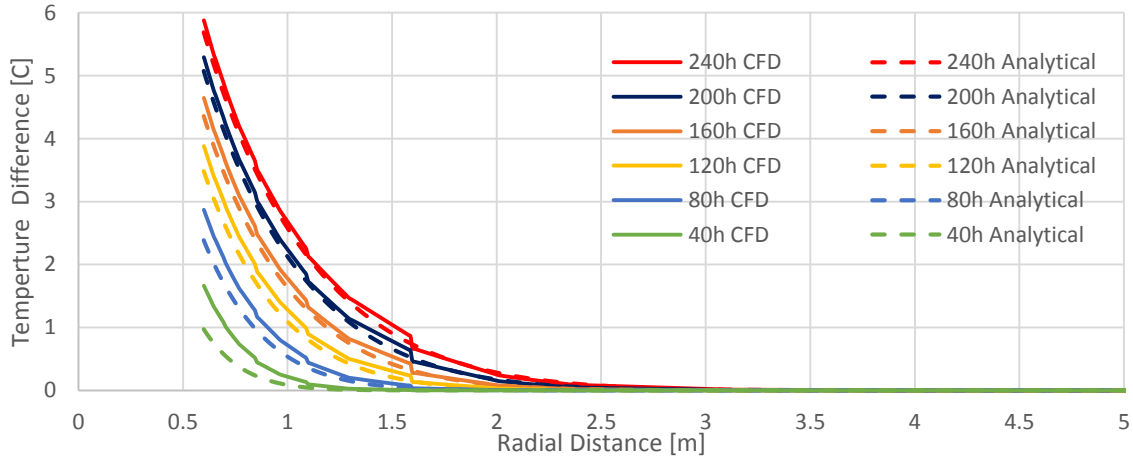

Figure 34: The 120cm 4 loop CFD and finite line source method radial temperature distribution/

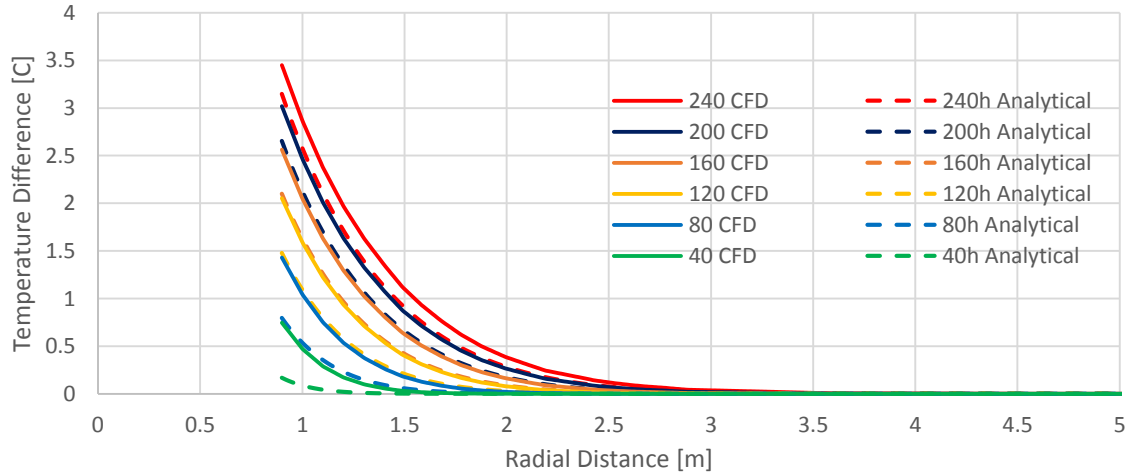

Figure 35: The 180cm CFD and finite line source method radial temperature distribution.

The finite line source method assumes a heat source as a line in a homogeneous medium, the piles tested in this comparison become less like a line source of heat as the pile diameter gets larger. The difference between the finite line source method and the large diameter piles was expected to become greater as the diameter of the pile gets larger. This finite line source comparison was made over the course of the simulation time of 240h, a relatively short time period in comparison to the steady state operation of GEP systems. The finite line source method underestimates the response of the pile at small time durations because it assumes that the heat source is at the center of the pile instead of close to the perimeter. The underestimation of the finite line source was greater with larger pile diameters because the heat is applied further away from the center of the pile as shown in Figures 33-35.

3.4 120cm Pile with different Loop Configurations

The loop configuration inside of a GEP can greatly affect the performance of a GEP but as shown in this comparison does not have as large an effect as changing the diameter of the pile. In this comparison a 120cm piles were compared with three different loop configurations. The pile is simulated with 4 loops, 5 loops, and 6 loops, all of the other parameters remain the same as explained above and shown in Tables 8 and 9. The geometry of the three 120cm piles is shown in Figure 36 with a top view of the pipe configurations shown in Figure 37. In each of the three configurations the HDPE pipes are equally spaced around the piles and the same distance from the pile surface. The number of loops is increased by one in each case adding two HDPE pipes to the pile.

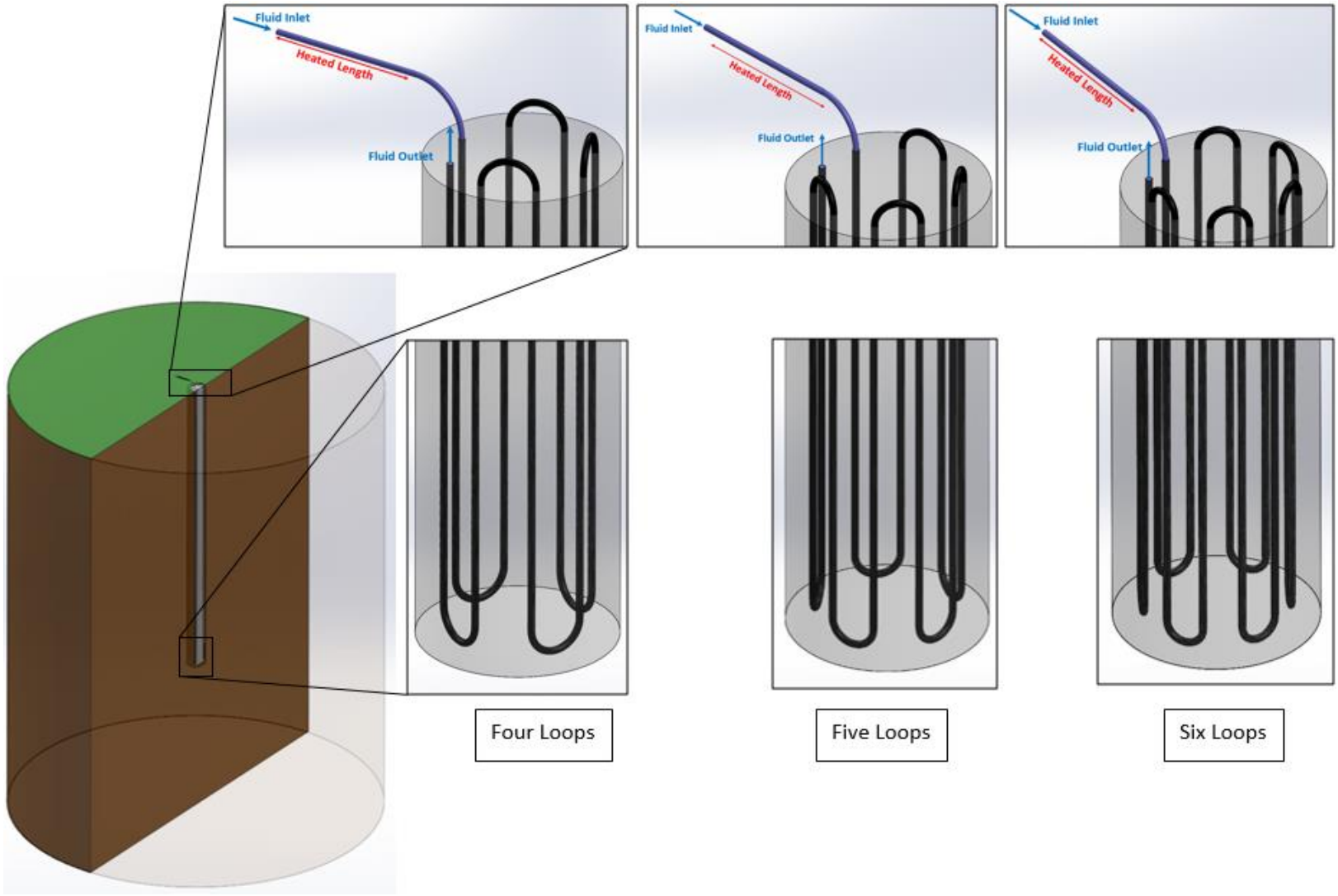

Figure 36: The geometry of the 120cm pile with 4, 5, and 6 loops with enlarged views of the loop configurations.

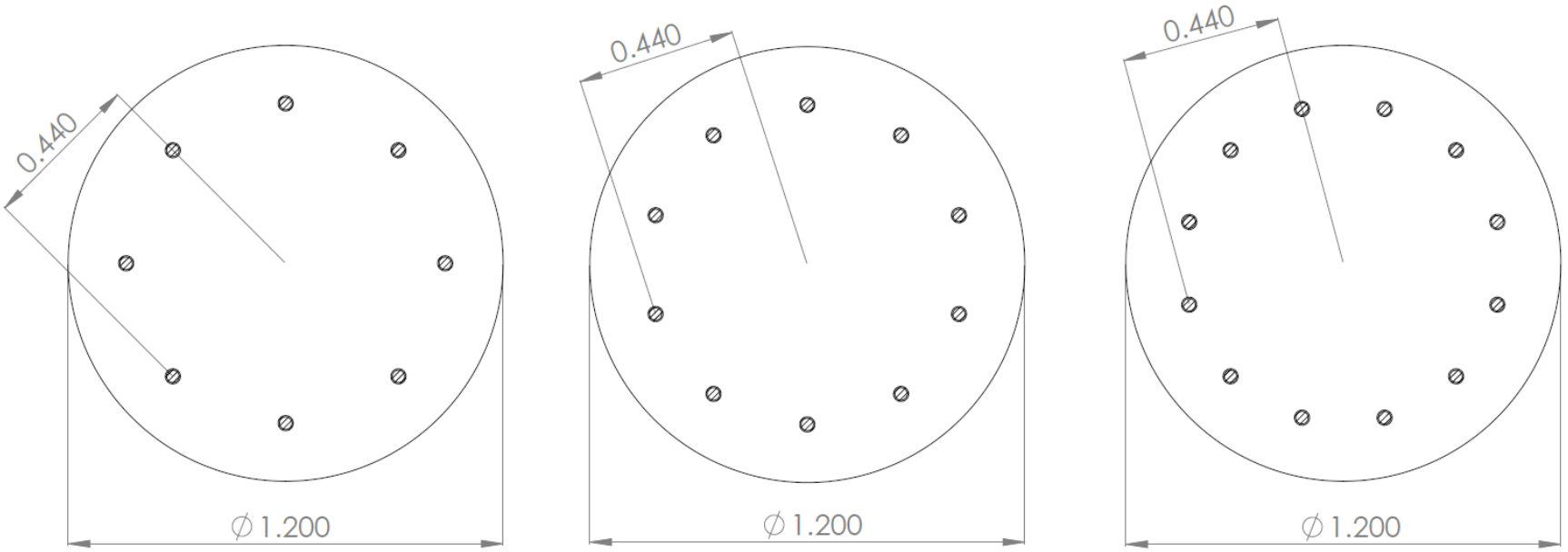

Figure 37: The loop configurations of the 120cm pile with 4, 5, and 6 loops, the number of loops increases by 1 with each case adding two HDPE pipes.

The temperature response of the three cases shows that each loop configuration responded similarly and were separated by approximately one half a degree Celsius from each other at the end of the 240 hour simulation. The temperature responses of the 120cm piles with 4, 5, and 6 loops is shown in Figure 38. The pile with a greater number of loops produced a lower temperature response because of the added heat transfer area within the pile. The additional heat transfer area allowed the input heat rate to be more effectively dissipated into the ground.

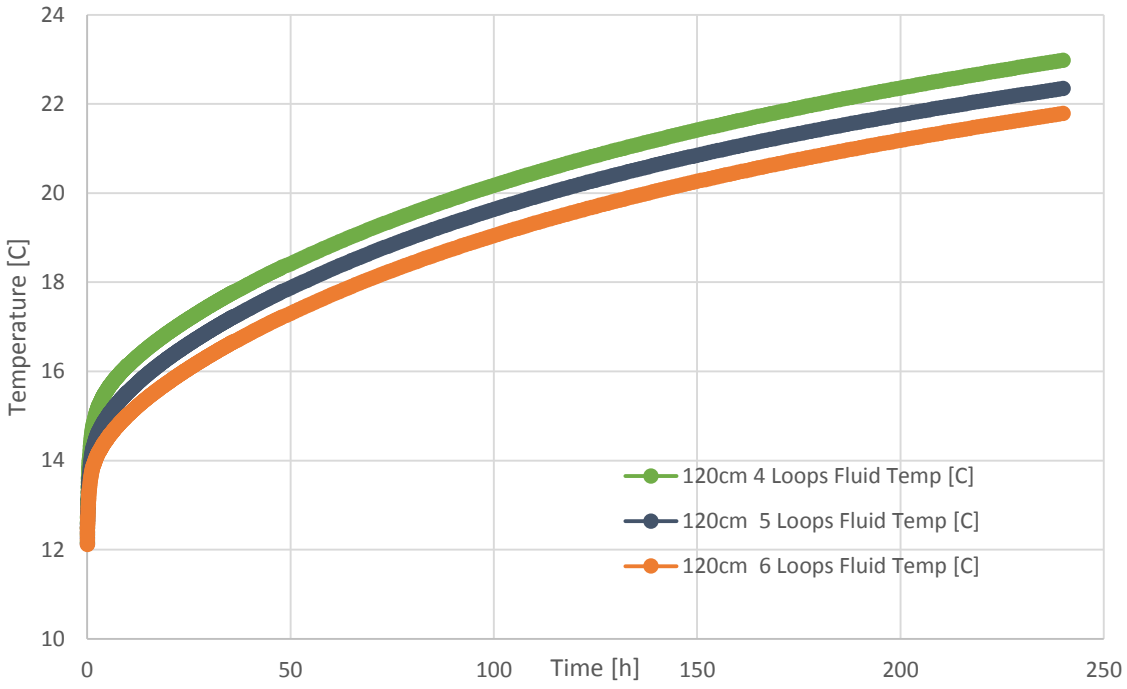

Figure 38: The temperature response of the 120cm pile with 4, 5, and 6 loops

The temperature response shown in a semi-log scale shows when the heat transfer rate has reached a steady state. When the temperature response develops a linear trend on a semi-log scale then the heat transfer through the system has reached steady state. The 120cm pile cases seem to be beginning a period of steady state heat transfer after 100 hours of operation. The same information as Figure 41 is shown in Figure 39 on a semi log scale.

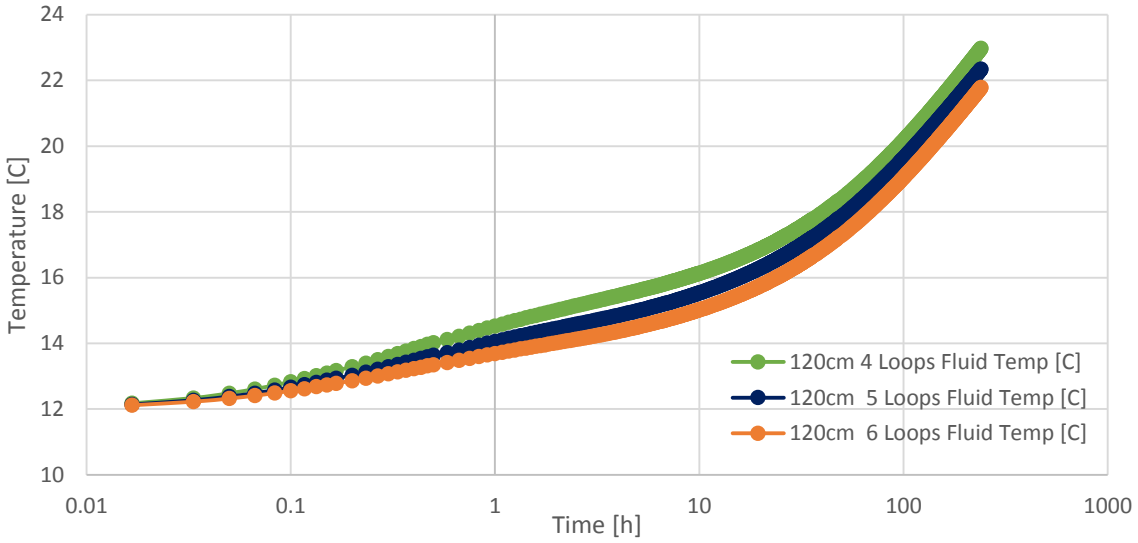

Figure 39: The temperature response of the 120cm pile with 4, 5, and 6 loops on a semi-log plot

The fluid heat flux for the three 120 cm pile cases shows that the fluid heat flux is nearly identical between the three cases. The total fluid heat flux or heat rate is shown in Figure 40 for the three 120cm piles. The total fluid heat flux into the HDPE pipe quickly approaches the input heat rate to the system after going through a large initial increase. Although the temperature values are slightly different between each case the temperature differential between the fluid and the HDPE pipe are insignificantly different between cases.

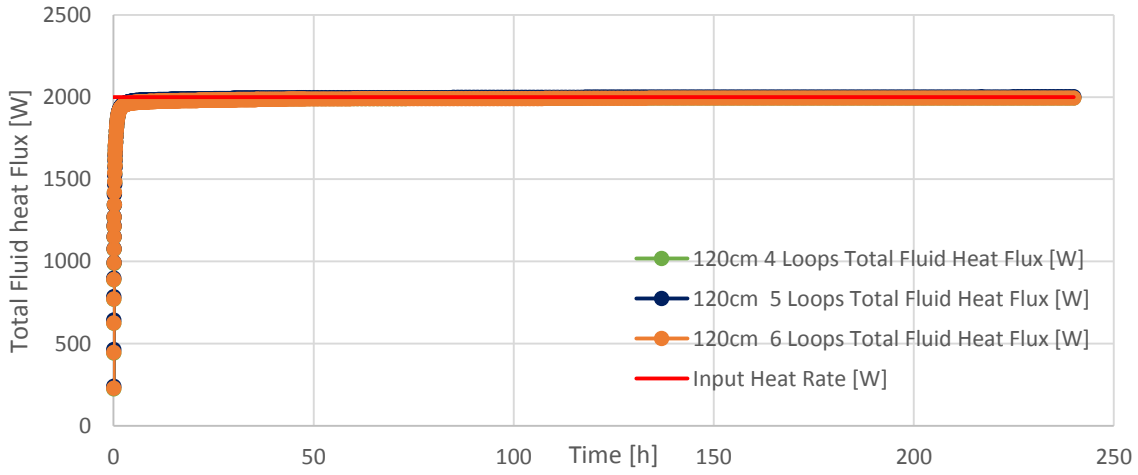

Figure 40: The total fluid heat flux of the 120cm pile with 4, 5, and 6 loops

The borehole heat flux of the three 120cm pile cases were also very similar to each other and respond with time at the same rate. The total pile heat flux for each 120cm pile is shown in Figure 41 for the duration of the simulation. This shows that the loop configuration does not affect the heat flux out of the pile like changing the diameter of the pile.

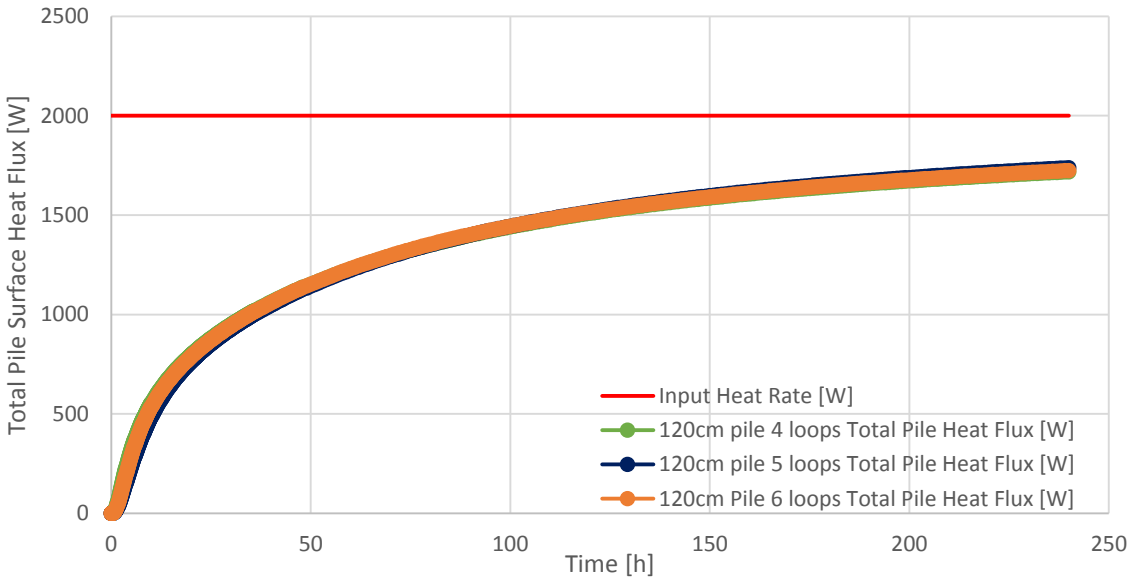

Figure 41: The total pile heat flux of the 120cm pile cases with 4, 5, and 6 loops

The pile resistance of the three 120cm cases shows that the more loops the pile had the lower the resistance of the pile. Pile resistance of the three 120cm piles is shown in Figure 42. Similar to the varying diameter cases the heat flux was essentially the same between cases and the pile length was a constant 20m so the temperature response of the fluid and the pile surface was the major contributor to the resistance of the pile. This comparison shows that the 120cm pile with 6 loops performs the best and was most effectively dissipate the input heat rate into the ground.

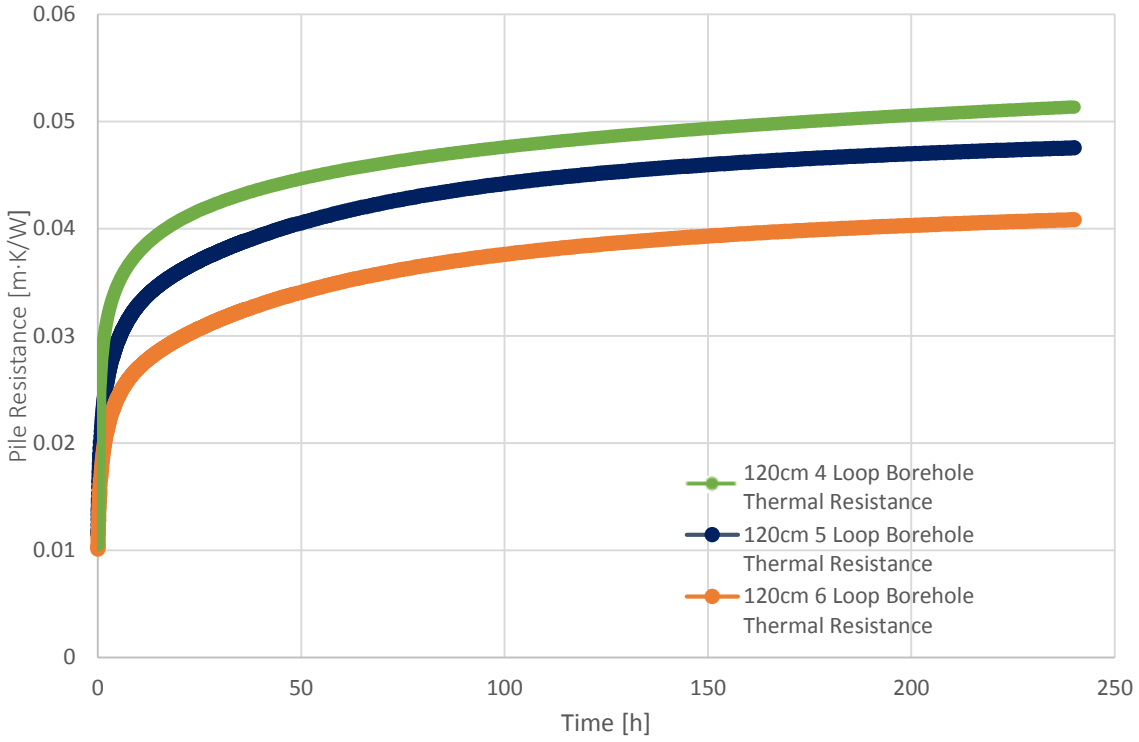

Figure 42: The pile thermal resistance of the 120cm pile with 4, 5, and 6 loops

The pile resistance decreased noticeably each time a loop was added to the circuit. Adding loops to a GEP increased its performance but in addition increased the total pressure drop of the fluid. The required pumping power to circulate fluid through the loop increased each time a loop was added to the circuit so that at a certain point the added heat transfer performance benefit would be outweighed by the increased energy needed to circulate the fluid through the GEP. Table 10 shows the total pressure drop through the pile for each loop configuration. The pressure drop was increased by approximately 600Pa for each loop added to the pile.

Table 10: The total pressure drop through each 120cm pile loop configuration.

Number of loops	*Pressure Drop Through the Pile [Pa]*
4	2476
5	3076
6	3669

The finite line source method was compared to the three 120cm pile cases in Figure 46. The CFD simulations of the 120cm piles all produced a greater temperature response than the finite line source method. The difference between the CFD and finite line source results was greatest at the beginning of the investigated time interval and became less as the time becomes greater. The finite line source data was only valid outside of the pile surface in the soil domain, this is why the data begins at 0.6m and not at 0. The 4 loop, 5 loop, and 6 loop configurations all produce similar radial temperature gradient results.

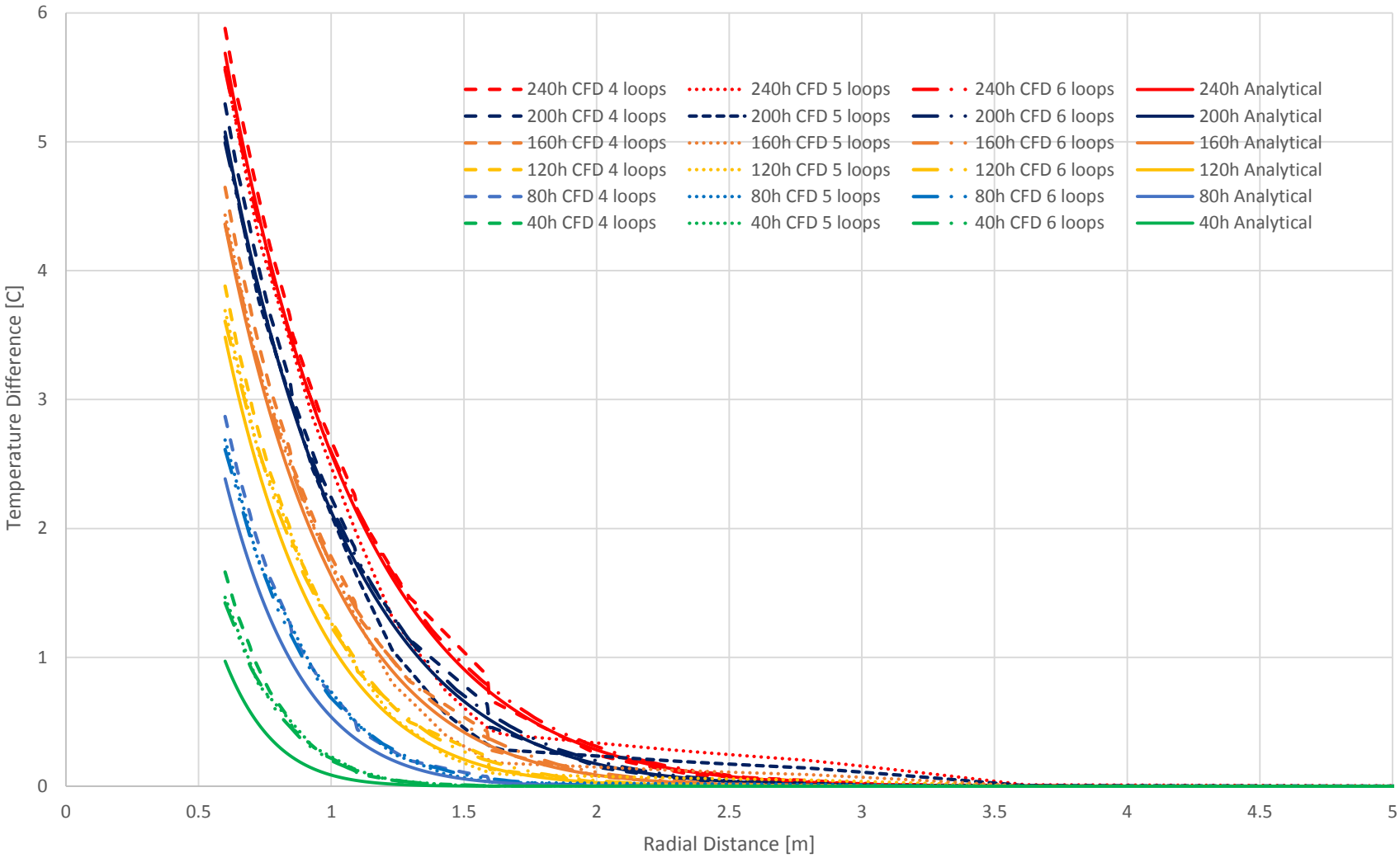

Figure 43: Radial temperature distribution comparison between the 120cm CFD cases and Line Source Method/

3.5 Large Diameter Conclusions

The large diameter pile systems were shown to offer an overall better performance as the pile diameter was increased in size and as the number of loops was increased. The more loops added to the system provides a greater effective heat transfer area for the system to dissipate the injected heat rate to the surrounding earth. The larger diameter piles also showed a greater ability to dissipate the heat in this comparison.

3.5.1 Varying Diameter Results

The 60cm, 120cm with 4 loops, and 180cm pile cases produced largely different results in the average fluid temperature response, total pile surface heat flux, and pile resistance. The average fluid temperature of the 60cm pile, 120cm with 4 loops, and 180cm pile reached an average fluid temperature value of 32, 23, and 19℃ respectively after 240 hours. This shows that the average fluid temperature 60cm pile and the 120cm pile with 4 loops increased 2.9 and 1.6 times as much as the 180cm pile. As the length of pipe within the pile and volume of the pile grew the pile performance increased. The temperature response of the fluid was less because of the increased distance between pipes and the larger heat transfer area between the fluid and the pile. These factors allowed the pile to more effectively absorb the input heat rate and dissipate it.

The heat rate through the pile surface of the 180cm pile reached 75% of the input heat rate after the full 240 hour simulation time. The 60cm pile and the 120cm pile with 4 loops reached 75% of the input heat rate through the pile surface after 31.5 hours and 117 hours respectively. This showed that the heat capacitance of the pile approached its maximum value much faster when the diameter of the piles were smaller. The heat flux

through the pile surface took a longer time to develop in the larger diameter piles because of the volume of the pile.

At the end of the 240 hour simulation the pile resistance of the three cases in order of increasing diameter were 0.096, 0.051 and 0.039 m·K/W. The 180cm pile resistance was 40% of the 60cm pile and 76% of the 120cm pile with 4 loops. These numbers clearly show that the 180cm pile more effectively dissipated the constant 2000W input heat rate to the surrounding soil over the course of 240 hours. The pile resistance is a measure of the average temperature difference between the pile surface and the fluid temperature. As the pile diameter increased the temperature response to the input heat rate decreased as a result the fluid temperature also stayed closer to the pile surface temperature. Piles with a smaller thermal resistance will maintain a fluid temperature closer to the undisturbed ground temperature.

The finite line source method was used to solve for the radial temperature distribution around the pile, this was compared to the results from the CFD simulation. This comparison shows that the finite line source method becomes increasingly unreliable as the diameter of the pile increases. As the diameter of the pile increases the pile geometry becomes less similar to a line. The finite line source method assumes the heat source is a line when in reality the heat source is applied near the perimeter of the pile. As a result the finite line source method produced less accurate results compared to the CFD simulation especially at low times. The line source comparison is especially important for developing testing standards for large diameter energy piles. The CFD results show a significant degree of error as the pile diameter gets larger in early times. The CFD results show that the line source method would produce inaccurate results for in-situ TRTs without

extending the test time beyond 10 days for the 180cm pile and beyond 7 days for the 120cm pile. Only a few cases are presented here but with a larger sample of test cases a standard could be developed for the recommended TRT test length based on the pile geometry.

3.5.2 Varying Loop Configuration Results

Changing the number of loops inside the 120cm pile did not affect the heat rate through the pile surface or through the fluid HDPE pipe interface. The average fluid temperature and the pile resistance were affected by the number of loops in the pile. The 4 loop, 5 loop, and 6 loop configurations had an average fluid temperature value of 22.9, 22.3 and 21.8℃ respectively. The difference in the average fluid temperature was significantly less from varying the loop configurations compared to varying the pile diameter. Adding one loop to the pile decreased the final average fluid temperature between 0.5 and 0.6℃. Each additional loop added to the pile decreased the temperature response by increasing the heat transfer area for the fluid to interact with the pile. The additional heat transfer area allowed more of the input heat rate to be dissipated within the pile and resulted in a lower temperature response. The pile resistance in order of least loops to most loops was 0.051, 0.048, and 0.041 m·K/W. The 120cm pile performed noticeable better as the number of loops was increased. The additional loops and heat transfer area decreased the pile thermal resistance by decreasing the temperature response of the fluid. The lower the temperature response of the fluid is, the closer to the pile surface and undisturbed ground temperature the fluid temperature will remain. This trend would be interesting investigate in order to discover how far the resistance could be lowered as more loops were added. Additional loops also increase the necessary pumping power needed, so any gained heat transfer performance of the loop could be offset by the need for

a larger circulation pump. In this case adding one loop to the pile increased the total pressure drop by approximately 600Pa. The line source comparison agreed with what was found in the varying diameter comparison that the line source method will become less reliable for larger diameter piles.

3.6 Recommendations for Future Study

The results of this study can assist in the development of standards and guidelines for large diameter energy piles. Industry standards improve the quality and cost effectiveness of systems and research should be continued in an effort to refine existing practices. The research in this paper can be continued by expanding the test matrix to incorporate more geometries and different independent variables.

The large diameter pile comparison study can be continued with a great deal of value added by extending the number of cases to the comparisons. Different diameter piles with more loop configurations can be tested to expand on the test matrix. These additional cases could be used to expand on the trends that were discovered. In addition to studying the diameter of the pile, a third dimension can be tested and the length of the pile can be varied to test longer or shorter piles. Testing variations in diameter, length, and loop configuration could significantly expand the research in this paper.

CFD analysis was used to simulate the large diameter piles in this paper because of the ability to expand the analysis into the fluid domain of the pile. The scope of this study was limited to the analysis provided but could be expanded. The same models can be used to test different flow rates and circulation fluids within the piles. Expanding the analysis into variations in the fluid also enables the convective heat transfer to be simulated and

tested. Investigating the effects of these variations on the geometry and flow characteristics leads to many possible new outlets for expanding this research.

References

References

[1] Sanner, B., Karytsas, C., Mendrinos, D., and Rybach, L., 2003, "Current status of ground source heat pumps and underground thermal energy storage in Europe," Geothermics, 32(4–6), pp. 579-588.
[2] Yang, H., Cui, P., and Fang, Z., 2010, "Vertical-borehole ground-coupled heat pumps: A review of models and systems," Applied Energy, 87(1), pp. 16-27.
[3] Lund, J. W., Freeston, D. H., and Boyd, T. L., 2011, "Direct utilization of geothermal energy 2010 worldwide review," Geothermics, 40(3), pp. 159-180.
[4] Mustafa Omer, A., 2008, "Ground-source heat pumps systems and applications," Renewable and Sustainable Energy Reviews, 12(2), pp. 344-371.
[5] McDaniel, M. L., 2011, "Proposed Design for a Coupled Ground-Source Heat Pump/Energy Recovery Ventilator System to Reduce Building Energy Demand," Virginia Polytechnic Institute and State University.
[6] Spitler, J., 2005, "Editorial: Ground-Source Heat Pump System Research—Past, Present, and Future," Hvac&R Research, 11(2), pp. 165-167.
[7] Ozgener, O., and Hepbasli, A., 2007, "A review on the energy and exergy analysis of solar assisted heat pump systems," Renewable and Sustainable Energy Reviews, 11(3), pp. 482-496.
[8] Hepbasli, A., and Akdemir, O., 2004, "Energy and exergy analysis of a ground source (geothermal) heat pump system," Energy Conversion and Management, 45(5), pp. 737-753.
[9] Lund, J. W., 1989, "Geothermal heat pumps-Trends and comparisons," Geo-Heat Center Quarterly Bulletin, 12(1), pp. 1-6.
[10] Loveridge, F., 2012, "The thermal performance of foundation piles used as heat exchangers in ground energy systems," University of Southampton.
[11] Adam, D., and Markiewicz, R., 2009, "Energy from earth-coupled structures, foundations, tunnels and sewers," Géotechnique, 59(3), pp. 229-236.
[12] Gehlin, S., 2002, "Thermal response test: method development and evaluation."
[13] BuilditSolar, 2013, "http://www.builditsolar.com/Projects/Cooling/EarthTemperatures.htm."
[14] Abdelaziz, S., Olgun, C., and Martin, J., 2011, "Design and Operational Considerations of Geothermal Energy Piles," Geo-Frontiers 2011© ASCE 2011.
[15] Florides, G., and Kalogirou, S., 2007, "Ground heat exchangers—A review of systems, models and applications," Renewable Energy, 32(15), pp. 2461-2478.
[16] Brandl, H., 2006, "Energy foundations and other thermo-active ground structures," Geotechnique, 56(2), pp. 81-122.
[17] Martin, J. R., Abdelaziz, S. L., and Olgun, C. G., 2010, "Renewable Energy Applications Using Thermo-Active Deep Foundations."
[18] Laloui, L., Nuth, M., and Vulliet, L., 2006, "Experimental and numerical investigations of the behaviour of a heat exchanger pile," International Journal for Numerical and Analytical Methods in Geomechanics, 30(8), pp. 763-781.

[19] Brettmann, T., Amis, T., and Kapps, M., 2010, "Thermal Conductivity Anlaysis of Geothermal Energy Piles," Proceedings of the Geotechnical Challenges in Urban Regeneration Conference. Deep Foundation Institute, London, UK, p. 6p.
[20] Brettmann, T., and Amis, T., "Thermal Conductivity Evaluation of a Pile Group Using Geothermal Energy Piles," Geo-Frontiers 2011, pp. 499-508.
[21] Witte, H. J., Van Gelder, G. J., and Spitler, J., 2002, "In situ measurement of ground thermal conductivity: a Dutch perspective," Ashrae Transactions, 108(1), pp. 263-272.
[22] Mogensen, P., 1983, "Fluid to duct wall heat transfer in duct system heat storages," Document-Swedish Council for Building Research(16), pp. 652-657.
[23] AUSTIN III, W. A., 1998, "Development of an in situ system for measuring ground thermal properties," Oklahoma State University.
[24] Eklöf, C., and Gehlin, S., 1996, "TED-a mobile equipment for thermal response test: testing and evaluation."
[25] Gehlin, S., and Nordell, B., 1997, "Thermal response test-a mobile equipment for determining thermal resistance of borehole," Proc. Megastock'97, pp. 103-108.
[26] Kavanaugh, S., Xie, L., and Martin, C., 2000, "Investigation of methods for determining soil and rock formation thermal properties from short-term field tests," ASHRAE Research Project(1118-TRP).
[27] Sanner, B., Hellström, G., Spitler, J., and Gehlin, S., "Thermal response test-current status and world-wide application," Proc. Proceedings world geothermal congress.
[28] GSHPA, 2011, "Closed Loop Vertical Borehole: Design, Installation & Materials Standards," (Issue 1.0).
[29] GSHPA, 2012, "Thermal Pile: Design, Installation & Materials Standards," (Issue 1.0).
[30] Ingersoll, L., and Plass, H., 1948, "Theory of the ground pipe heat source for the heat pump," ASHVE transactions, 47(7), pp. 339-348.
[31] Carslaw, H. S., and Jaeger, J. C., 1959, Conduction of heat in solids, Clarendon Press, Oxford,.
[32] Zeng, H., Diao, N., and Fang, Z., 2002, "A finite line-source model for boreholes in geothermal heat exchangers," Heat Transfer—Asian Research, 31(7), pp. 558-567.
[33] Incropera, F. P., and DeWitt, D. P., 2002, Fundamentals of Heat and Mass Transfer, John Wiley & Sons Incorporated.
[34] Moran, M. J., and Shapiro, H. N., 2008, Fundamentals of engineering thermodynamics, Wiley. com.
[35] Zeng, H., Diao, N., and Fang, Z., 2003, "Heat transfer analysis of boreholes in vertical ground heat exchangers," International Journal of Heat and Mass Transfer, 46(23), pp. 4467-4481.
[36] Anderson, J., "Computational Fluid Dynamics: The Basics with Applications. 1995," McGrawhill Inc.
[37] ANSYS, 2010, "ANSYS CFX-Solver Theory Guide," ANSYS CFX Release, 13.0.
[38] ASTM-Standard-D5334, 2008, "Standard Test Method for Determination of Thermal Conductivity of soil and Soft Rock by Thermal Needle Probe Procedure," ASTM International.
[39] Ozudogru, T., Senol, A., Olgun, C. G., James R. Martin, I., and Brettmann, T., "Thermal Conductivity Testing of Energy Piles: Field Testing and Numerical Modeling," GeoCongress 2012, pp. 4436-4445.

[40] Multiphysics, C., 2010, "4.1 User Guide," Stockholm, Sweden.
[41] ANSYS, 2009, "Meshing Help Release 12.1," Canonsburg, PA.
[42] Markiewicz, R., 2004, "Numerical and experimental investigations for utilization of geothermal energy using earth-coupled structures and new developments for tunnels," Doctoral Thesis, Vienna University of Technology.
[43] Brown, D., Turner, J., and Castelli, R., 2010, "(2010). Drilled Shafts: Construction Procedures and LRFD Design Methods," FHWA NHI-10-016, May.